Review

The emergence of nanocellulose aerogels in CO$_2$ adsorption

Farida Baraka, Jalel Labidi [*]

Biorefinery Processes Group, Chemical and Environmental Engineering Department, Engineering Faculty of Gipuzkoa, University of the Basque Country UPV/EHU, Plaza Europa 1, 20018 Donostia, Spain

HIGHLIGHTS

- Nanocellulose aerogels are promising adsorbent to capture CO$_2$.
- Supercritical drying used for synthesizing nanocellulose-based aerogels is inherently energy intensive.
- Functionalization of nanocellulose aerogels with amines improves the adsorption rates of CO$_2$.
- Development of new processing technologies is required to reduce production costs.

GRAPHICAL ABSTRACT
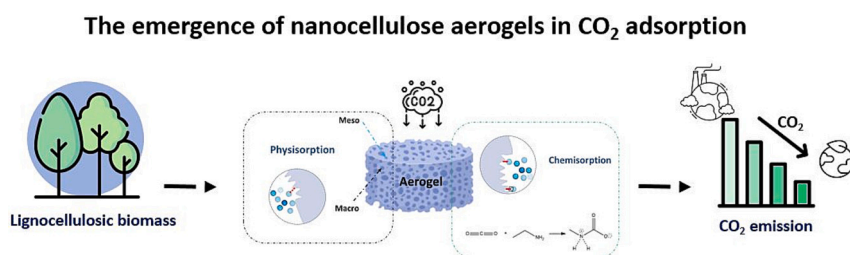
ARTICLE INFO

ABSTRACT

Mitigating the effect of climate change toward a sustainable development is one of the main challenges of our century. The emission of greenhouse gases, especially carbon dioxide (CO$_2$), is a leading cause of the global warming crisis. To address this issue, various sustainable strategies have been formulated for CO$_2$ capture. Renewable nanocellulose aerogels have risen as a highly attractive candidate for CO$_2$ capture thanks to their porous and surface-tunable nature. Nanocellulose offer distinctive characteristics, including significant aspect ratios, exceptional biodegradability, lightweight nature, and the ability for chemical modification due to the abundant presence of hydroxyl groups. In this review, recent research studies on nanocellulose-based aerogels designed for CO$_2$ absorption have been highlighted. The state-of-the-art of nanocellulose-based aerogel has been thoroughly assessed, including their synthesis, drying methods, and characterization techniques. Additionally, discussions were held about the mechanisms of CO$_2$ adsorption, the effects of the porous structure, surface functionalization, and experimental parameters. Ultimately, this synthesis review provides an overview of the achieved adsorption rates using nanocellulose-based aerogels and outlines potential improvements that could lead to optimal adsorption rates. Overall, this research holds significant promise for tackling the challenges of climate change and contributing to a more sustainable future.

1. Introduction

A viable strategy to overcome climate change, is to decrease the emission of carbon dioxide (CO$_2$), the main Earth's greenhouse gas responsible for the global warming. CO$_2$ is primarily produced by human activities, including the combustion of fossil fuels (in transport, industry, food processing, housing, etc.), agriculture and deforestation. Although the natural greenhouse effect is essential to maintaining living conditions on Earth, the progressive buildup of greenhouse gases in the atmosphere is initiating a rise in global temperatures. Since the

beginning of the industrial era, the level of CO_2 emissions has steadily increased each year with the exception of a notable reduction in 2020 due the COVID-19 pandemic, as shown in Fig. 1 (CO₂ emissions | Energy economics | Home, n.d.). However, this sharp decrease in carbon emissions was only temporary. As soon as the restrictions related to COVID-19 were smoothed and the industrial activities totally resumed, greenhouse gas emissions have risen to unprecedented levels. This sharply increases in emissions, closely correlated with fossil fuels consumption, highlights the fragility of the system and underscores the urgent need for actions. Therefore, to overcome global warming and reach a net-zero emissions strategy, it is crucial to implement economically viable CO_2 capture technologies worldwide. This will require significant investment and innovative approaches to develop effective, sustainable solutions that can be widely adopted.

Carbon dioxide capture and storage (CCS) is recognized as a pivotal strategies to effectively minimize and recycle CO_2 emissions (Bui et al., 2018). CCS involves the selective capture of CO_2 during energy conversion or industrial processes, succeeded by compression, transportation, and permanent storage of the captured CO_2. CCS includes three main methods: pre-combustion, post-combustion and oxy-combustion (Kanniche et al., 2010). Pre-Combustion consists in the capture of CO_2 directly from the conversion of a synthesis gas composed mainly of carbon monoxide (CO) and hydrogen. Post-combustion corresponds to the treatment of exhaust gases after the fuel has been completely burned with air. Oxy-combustion strategies involve the fuel has undergone complete combustion with air. Many strategies have been employed to separate CO_2 from a gas mixture including absorption (Wang et al., 2011), adsorption (Wörmeyer et al., 2012), membranes (Powell and Qiao, 2006) and cryogenic separation (Hart and Gnanendran, 2009). While CO_2 capture technologies are essential for addressing climate change, many of the current methods come with economic and environmental drawbacks, highlighting the need for green, cost-effective capture strategies. Among the technologies currently available, adsorption, a surface energy phenomenon, appears as the most convenient method for an economical large-scale development (Sai Bhargava Reddy et al., 2021).

The solid adsorbent separation consists in the adsorption of a specific gas on a solid surface. The success of this method mainly relies on the development of a powerful adsorbent with high selectivity and adsorption capacity (Kong et al., 2016). Adsorption is essentially based on the interaction between the adsorbate gas and the substrate surface, which can occurs through weak interactions, i.e. physical adsorption,

such as Van der Waals and dipolar interactions or strong interactions, i. e. chemical adsorption, via covalent chemical bonds (Kecili and Hussain, 2018). In physical adsorption, the adsorbent can be reused over several cycles adsorption, desorption, and regeneration of the adsorbed surfaces. In chemical adsorption exhibits a higher adsorption rat, however the regeneration of the adsorbent proves to be difficult, which limits the scope of applications. Therefore, the development of adsorbents combining physical and chemical adsorption processes seems to be an interesting approach. A wide range of advanced functional materials for CO_2 adsorption have been developed, such as activated carbon (Ogungbenro et al., 2017), organic polymers (Yaqub et al., 2016), zeolites (Chen et al., 2017), metal-organic frameworks (MOF) (Belmabkhout et al., 2016), and metal oxides (Bhatti et al., 2018).

However, these adsorbents are predominantly sourced from fossil resources, and a majority of them encounter challenges related to intricate equipment, usage of toxic reagents, significant susceptibility to corrosion, and limited production capacity. Aerogel materials has become in recent years an attractive alternative to these conventional adsorbents (Keshavarz et al., 2021). Aerogels represent three-dimensional (3D) highly porous substances created from organic, inorganic, or hybrid molecular precursors. These aerogels are typically synthesized using a sol-gel process combined with appropriate drying methods (Husain et al., 2021). They are categorized by a very large surface area, a low density, and strong mechanical properties, which makes them highly effective for CO_2 adsorption and storage purposes. Firstly reported in 1994 by Huang et al. (1994), silica gels stand for the first aerogels developed for CO_2 adsorption. Later, Ahmed et al. developed in 1998 aerogels containing calcium and magnesium oxides (Ahmed and Attia, 1998). Since then, extensive study was conducted on the synthesize of alternatives aerogels for CO_2 adsorption including polymer aerogels based on polyimide (Meador et al., 2012), polyurethane (Rigacci and Achard, 2011), polyvinylchloride (Yamashita et al., 2003), and poly(vinyl alcohol) (Cheng et al., 2018). Nevertheless, the extensive application of these materials as effective agents for CO_2 adsorption remains constrained by their comparatively inadequate thermal and chemical stability, limited specific surface area, and the high costs associated with their production (Wei et al., 2022). Hence, there is still a need for the design of more efficient, economical, and sustainable adsorbents for CO_2 capture. Bio-based aerogels are a promising new class of environmentally friendly materials having the potential to replace conventional non-biodegradable materials such as silica or petroleum-based polymers in the long-term storage of CO_2
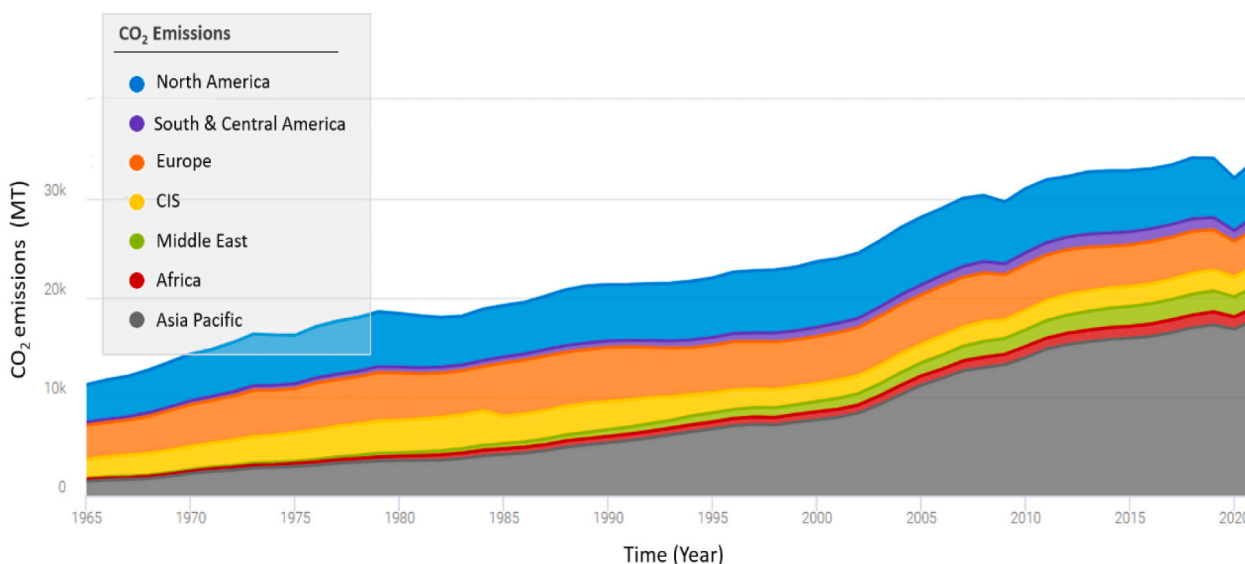

Fig. 1. Global greenhouse gas emissions from 1965 to 2020. Adapted from (Economics, Statistical Review of World Energy, n.d.).

captured (Verma et al., 2020).

Significant endeavors have been focused on the development of bio-based aerogels, leading to the conception of efficient CO_2 capture adsorbents such as chitin (Dassanayake et al., 2018), chitosan (Song et al., 2018), and cellulose based aerogels (Ho and Leo, 2021). Aerogels derived from cellulose are particularly attractive, as they are sourced from renewable lignocellulosic biomass and demonstrate exceptional mechanical properties (Illera et al., 2018). Cellulose, the most profuse natural polymer on nature, can be extracted from renewable resources like wood, cotton, or hemp (Chen, 2014). Nanocellulose, the nano structure of cellulose, combines the important properties of the biopolymer, including high specific resistance and hydrophilicity, with the specific properties of nanometer-scale materials (Xu et al., 2022). According to the morphology obtained after their isolation, nanocelluloses can be categorized into three primary groups: (1) cellulose nanofibers (CNFs), (2) cellulose nanocrystals (CNCs), and (3) bacterial nanocellulose (BNC). Nanocellulose-based aerogels can be easily prepared by a pulp nanofibers mixing step followed by a gelation process using a small amount of a crosslinking agent (Chen et al., 2021). The resulting soft and porous aerogel materials exhibit high surface areas, low densities, and good mechanical stability (Wei et al., 2020). To enhance their performance, cellulose-based aerogels have undergone modifications involving the introduction of amine functional groups. This modification enhances their ability to capture CO_2 and facilitates the creation of exceptionally selective and durable monolayers (Ho and Leo, 2021). Among these modifications, the integration into inorganic matrices to create hybrid systems appears to be a promising approach, leading to a significant enhancement in adsorption rate (Rostami et al., 2022).

Considering the substantial expansion of nanocellulose-based aerogel research, a comprehensive review of previous studies on these adsorbents becomes paramount for the development of sustainable CO_2 capture strategies. The aim of this study is to provide a comprehensive review of nanocellulose-based aerogels, covering their synthesis methods and characterization. It will also address the adsorption mechanism, including the application of kinetics and isotherms models to quantify adsorption capacity, as well as the examination of factors influencing it. In addition, the review will explore the process of enhancing nanocellulose-based aerogels through functionalization and their incorporation into inorganic materials to increase their adsorption capacity. Finally, a comprehensive perspective and approaches to enhance the CO_2 adsorption capacity in nanocellulose aerogels have been presented, providing an understanding of current developments and future research directions.

2. Aerogels overview

Aerogels are a specific class of porous materials where the sol (liquid) part is substituted by a gas without shrinking their shape (Pierre and Pajonk, 2002). They are formed by exposing a wet gel precursor to a critical drying point to eliminate the liquid phase by supercritical drying. These advanced ultralight and highly porous materials retain gas, usually air, in the shape of pores or solid networks. This aerogels are characterized by unique properties, including lightness, low density, large surface area, and high mechanical strength, making them suitable for several applications (Keshavarz et al., 2021).

The shapes and sizes of aerogels can be adjusted depending on their final applications. They can be classified according to their appearance as monolith, powder, or film as reported in Fig. 2. They can be also classified as microporous (Ø = 2 nm), mesoporous (Ø = 2–50 nm) and macroporous (Ø > 50 nm) aerogels based on the pore's structures. The aerogel's chemical composition (inorganic, organic, or composite systems) drive the aerogel's final properties. Inorganic aerogels are all oxides, such as silica (SiO_2) (Lin et al., 2021), alumina (Al_2O_3) (Zu et al., 2013), titania (TiO_2) (Campbell et al., 1992), zirconia (ZrO_2) (Walker et al., 2021), or mixed oxides such as mullite (Song and Zhao, 2018). These materials generally exhibit low strength and a tendency to collapse easily when subjected to low stress. Organic aerogels are made from organic precursor products such as phenolic formaldehyde resin (Lee and Park, 2020), or more recently from biopolymers. These innovative materials are developed from renewable and abundant bioresources, such as cellulose, chitosan, alginates, or proteins. They offer high physical properties with reduced environmental impact (Verma et al., 2020). Composite aerogels are generally composed of mixed oxides or metal oxides, and can also be produced by a mixture of inorganic and organic precursors (Liu et al., 2020).

Aerogels can be grouped into two categories according the types of sol-gel processing. The formation of a sol-gel can be produced through the classical method developed by Kistler et al. in his pioneer work on aerogels (Kistler, 1931), currently applied for all oxide-based aerogels. The sol-gel synthesis method involves dissolving monomers in a solution, resulting in numerous interactions through hydrolysis and polycondensation reactions, ultimately leading to the formation of oligomers and particles that intricately interconnect to create a three-dimensional network. The second approach involves the dissolution of polymers to form a highly diluted polymer solution. The swelling of the polymer lead to the rearrangement of its chains to obtain a 3D gel structure. The dissolving agent is then removed by cooling techniques, i.e. freeze-dryer (Jiménez-Saelices et al., 2017).
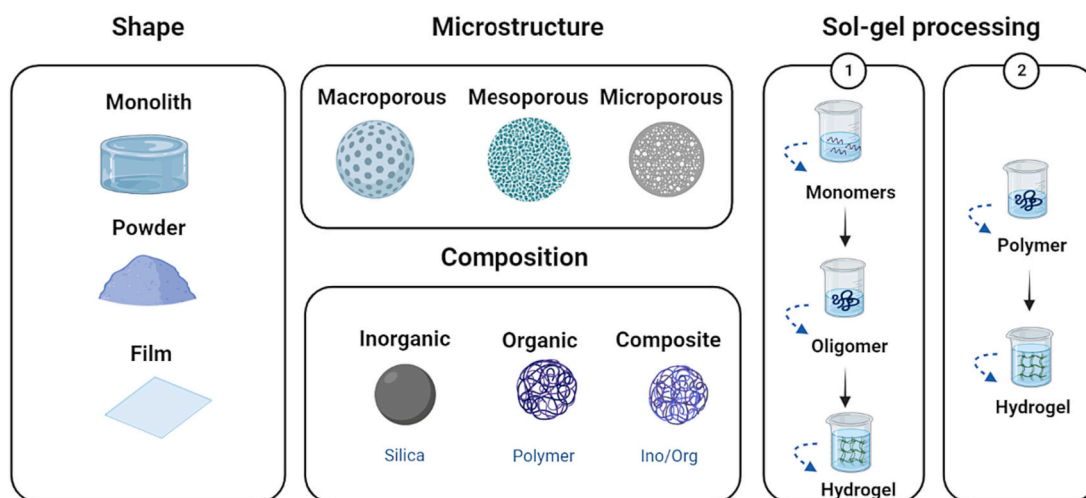

Fig. 2. Classification of aerogels.

3. Emergence of nanocellulose-based aerogel

Aerogels were identified and brought to light by Kistler early in the 1930s at the College of the Pacific in Stockton, California (KISTLER, 1931). According to his preliminary studies, the elimination of the liquid phase from a suspension can occur without disrupting the structure, achieved through the creation of liquid-vapor interfaces at a defined critical point. This technique was employed for nearly 30 years to produce aerogels solely from silica. In the 1960s aerogels were fabricated by Teichner and Nicolaon using the frequently employed sol-gel method (Teichner et al., 1976). The term sol-gel refers to solid nanoparticles dispersed in a liquid (a sol) agglomerate to form a continuous three-dimensional interconnected network (a gel) (Reichenauer, 2011). This new easy, fast and efficient methodology allowed the development of a series of new aerogels, exhibiting simultaneously the specific proprieties of the starting material and the characteristic features of the final aerogel. Aerogels are prepared from a wide variety of materials including metal oxide (Teichner et al., 1976), carbonaceous materials (Wu and Xu, 2014), polymer-based (Meador et al., 2012), and more recently naturally occurring feedstocks (Verma et al., 2020).

In recent decades, considerable effort has been dedicated to develop innovative materials using renewable and abundant bio-resources (Verma et al., 2020). In fact, awareness of using expensive, toxic, and fossil-based materials is driving researchers to develop innovative economical, benign, and green materials. A wide range of biopolymers, including alginate, cellulose, lignin, pectin, chitosan, proteins, and other sources, have undergone thorough assessment as potential precursors. These materials are carbon neutral, sustainable, renewable, recyclable, non-toxic, biodegradable, and biocompatible (Wang et al., 2019). The inherent characteristics of biopolymers, coupled with the distinctive three-dimensional frameworks of aerogels, have unveiled fresh and appealing possibilities for potential applications.

With an annual output of approximately 200 billion tons, cellulose stands as the most abundant renewable resource on earth (Mankar et al., 2021). It is the main structural component of plant cell walls and confers them mechanical strength and chemical stability. It is a linear carbohydrate homopolymer formed by D-glucose units linked together by β-1,4 bonds. Through their strong inter- and intra-chain Van der Waals hydrogen bonding, compact cellulose fibrils are formed, which can be oriented differently, resulting in various levels of crystallinity (Ummartyotin and Manuspiya, 2015). Cellulosic materials with a dimension in the nanometer range are generally referred as nanocellulose. Nanocelluloses combine the important properties of cellulose, such as high specific strength, biodegradability, biocompatibility, and hydrophilicity, with the specific characteristics of nanoscale materials (Moon et al., 2011).

The evolution in nanotechnology turns the extraction of nanoscale structured materials from cellulose into a worldwide challenge. Nanocellulose, the nanoscale fibrillary crystalline domains derived from cellulose, is generally classified in three types: cellulose nanocrystals (CNCs), bacterial nanocellulose (BNC), and cellulose nanofibrils (CNFs) (Moon et al., 2011). CNCs are composed by crystalline cellulose fragments, in which amorphous regions are specifically eliminated via acid hydrolysis of glycosidic bonds. BNC originates from the transformation of glucose molecules into cellulose nanofibrils through various bacterial species. CNFs are thread-like fragments encompassing both amorphous and crystalline domains. It usually synthesized using several mechanical extraction processes involving microfluidization, grinding, and ultrasonication (Nagarajan et al., 2020).

3.1. Synthesis of nanocellulose aerogels

Nanocelulose-based aerogels are produced in a series of well-defined stages. The production includes the following procedures: (i) nanocellulose dispersion, (ii) gelation of nanocellulose, (iii) elimination of solvent (ambient drying, freeze drying, or supercritical drying) preceded by solvent exchange.

3.1.1. Dispersion and gelation of nanocellulose

The preparation of nanocellulose hydrogels involves dispersing of nanocellulose in water, achieved through ultrasonic or mechanical techniques. Nanocellulose has a well-defined crystalline structure, enriched in surface with hydroxyl groups subjected to strong inter- and intramolecular hydrogen bonds (Xiao et al., 2015). These chemical interactions contribute to the self-aggregation and the entanglement of cellulose nanocrystals (CNCs) or cellulose nanofibrils (CNFs). Therefore, the dissolution of CNCs or CNFs in water, lead to a 3D network formed through hydrogen bonding and entanglement of long fibrils. A more stable aqueous dispersion can be formed via electrostatic repulsion by introducing negatively charged groups onto the nanocellulose surface (Fall et al., 2011). These charges allow an increase of the hydrogel modulus, thus avoiding shrinkage during the drying process, even at low nanocelullose content (Chen et al., 2021). The gelation process leads to the formation of a linked polymer network (Liebner et al., 2007). The ultimate structure and the speed of hydrogel formation predominantly depend on the type of cross-links (whether chemical or physical) established among the cellulosic chains (van de Witte et al., 1996). The physical cross-links consist in weak forces such as van der Waals forces, hydrogen bonding, and hydrophobic or electronic Interactions (Benselfelt and Wågberg, 2019). Chemical cross-linking is initiated by introducing specific agents into the solution, where they engage in reactions with nanocellulose, leading to the establishment of covalent bonds (Liu et al., 2017). This process can be triggered by various methods, including radical polymerization, UV irradiation, Schiff base formation, addition, condensation, or enzymatic reactions (De France et al., 2017).

3.1.2. Drying strategies of nanocellulose aerogels from hydrogel

The drying process is designed to remove the liquid located inside the pores. The main issue of this step is to maintain the geometry of the wet gel and preventing the disruption of the network formed as a result of bending of the air-liquid interface. Indeed, the water present in the pores exhibits a relatively high surface tension resulting in a high capillary pressure on the pore walls at the gas-liquid interface. Consequently, solvent's evaporation may induce the collapse and the destruction of the pores (Scherer, 1986). Thus, by decreasing the capillary pressure (P) calculated according to the Young-Laplace equation, it is possible to limit the shrinkage (Eq. (1)). To this aim, water can be replaced with a solvent presenting a lower surface tension (γ), the pore radius (θ) can be reduced through an increase of the pore size (r), or even enhanced the mechanical properties of the pore walls to obtain well-structured materials.

$$P = \frac{-2\gamma cos\theta}{r} \tag{1}$$

Several drying techniques have been developed to eliminate the solvent in the pores, while producing a highly porous aerogel network as showed in Fig. 3.

3.1.2.1. Freeze-drying.
The freeze-drying process produces open pore foam materials, often referred to as "cryogels", that differs from aerogels as the porosity is not mainly framed in the mesoporous range (Buchtová and Budtova, 2016). This drying method consists in the sublimation of solid, i.e. frozen water, from the nanocellulose hydrogels pores (Jiménez-Saelices et al., 2017). Drying through sublimation avoids the formation of a liquid/vapor interface and prevent high capillary pressure that could deform or collapse the porous structure (Deville, 2010). The freeze-drying technique is performed as follows: i) the liquid contained in the wet gel is frozen, ii) the pressure is decreased, iii) the frozen water inside the pores is sublimated resulting in an interconnected porous structure. The nanocellulose concentration, the shape and the size of the gel govern the sublimation rate of the liquid present in the
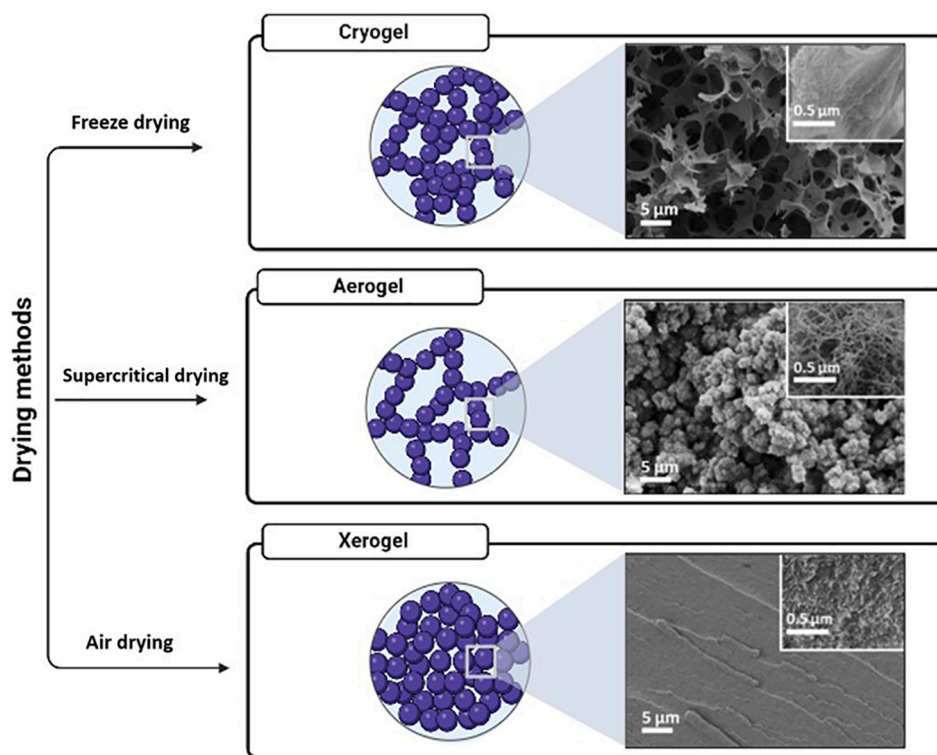
Fig. 3. SEM images of cryogel, aerogel and xerogel made from nanocellulose. Adapted from (Buchtová and Budtova, 2016) with permission.

pores (Liu et al., 2021). However, the morphology and pores distribution of the cryogels mainly depends on the growth of ice crystals in the pores which depend on the cooling rate and the crystallization temperature (Lavoine and Bergström, 2017). Rapid freezing of the solvent, otherwise called homogeneous freezing, corresponds to the immersion of the aqueous nanocellulose gel suspension in a liquid nitrogen bath by unidirectional ice shaping. This outcomes in the controlled orientation and growth of ice crystals, allowing to preserve the structure of the original dispersion. The sublimation of the crystals following homogeneous freezing leads to cellular foams with a 3D cellular structure, commonly called isotropic foams characterized by small pores sizes and a high surface area (Martoia et al., 2016). A slower freezing of the solvent, otherwise called ice templating (IT), leads to the segregation of the solvent and a dispersed phase during the crystal growth. This affects the intrinsic structure of the wet dispersion which leads to very low porosity honeycomb structures characterized by the larger pores aligned parallel to the freezing direction (Munier et al., 2016). The freeze-drying is an environmentally friendly and economically viable technique; allowing its use for cryogels production at an industrial scale. However, the formation of microcrystals, which turn out to be the dominant structural element, alters the fine structure of the gel therefore inhibiting the development of a mesoporous network known as aerogel (Buchtová and Budtova, 2016).

3.1.2.2. Supercritical drying. The supercritical drying technique is employed for the development of high added-value, ultra-light and porous aerogels (Lavoine and Bergström, 2017). This technique has been widely demonstrated to be suitable for the development of highly porous products, requiring no additional purification steps, using supercritical carbon dioxide, and fulfilling industry quality and safety standards (Rollins et al., 2002). The supercritical conditions imply the vanishing of the gas-liquid interface, thus avoiding pores collapse while keeping the porous structure of the wet gel intact. Due to the low solubility of water in Sc-CO_2, an organic solvent exchange is required before supercritical drying. Wet gels are often submerged in ethanol or acetone that are

miscible with Sc-CO_2. This immersion impedes the production of capillary pressure during solvent removal. In brief, supercritical drying consists in placing the wet gel in a closed and preheated autoclave. Then the autoclave is filled with carbon dioxide. The pressure and temperature must exceed the critical temperature and pressure of the solvent trapped in the gel pores. By increasing the pressure, the solvation power of CO_2 increases, making the liquid and vapor phases a single and unique phase. Once the pores have been drained by the organic solvent, the autoclave is depressurized by opening the outlet valve to collect the aerogel. Compared to other drying methods, the supercritical drying technique produces nanocellulose aerogels with higher specific surface area and lower shrinkage. Zang et al. prepared nanocellulose based aerogel via two different drying techniques to examine the effect of drying methods on the performance of CNFs aerogels (Wang et al., 2020). The drying methods yielded materials with different porous structures. CNFs aerogels produced by freeze-drying exhibited higher shrinkage, lower specific surface area, and higher pores volume as compared to supercritical drying. Although improved nanocellulose aerogels can be developed via the supercritical drying route, long processing time, large amount of waste solvent, and high cost production, may constitute a roadblock to the aerogel manufacture at the industrial scale.

3.1.2.3. Ambient drying. Ambient pressure drying corresponds to the evaporation of the interstitial liquid of wet gels at ambient condition. The resulting matrices, referred as "xerogels", exhibit meso- and microporous structures, showcasing high porosity up to 50 %. The low density originates from the shrinkage of the network caused by the liquid meniscus and the pressure gradient. In fact, the radius of the liquid-vapor interface decreases following the evaporation of the solvent from the pores. This induced pressure on the pore walls leads to the collapse and the shrinkage of the network. The high capillary pressure can be reduced using solvent with low interfacial surface tension, i.e. ethanol, acetone, or pentane (Svensson et al., 2013). However, since the gels are made of nanocellulose with strong intramolecular hydrogen

bonds, the pressure will be high resulting in further damage to the gel structure. Otherwise, the contact angle between the interstitial liquid and the pore walls can be reduced by hydrophobizing the nanocellulose surface. In the 1990s, low density silica xerogels were produced by Deshpande et al. (1992). The chemical modification of the gel pore surface by silylation does not lead to a significant collapse of the pores responsible for high densification. Indeed, during the evaporation of silylated silica gels, a phenomenon referred to as 'springback' effect take place. Initially, the gel contracts and subsequently nearly returns to its original volume as the solvent front recedes. This behavior is attributed to the non-condensable species on the pore walls, preventing covalent bridging. Inspired by the work done on silica-based xerogels, G. Pour et al. have developed cellulose xerogels with high hydrophobicity (Pour et al., 2015). The esterification of the cellulose using trityl chloride avoided shrinkage. The resultant material exhibited significant porosity and low density, comparable to cellulose aerogels derived through supercritical drying. In summary, ambient drying stands out as a straightforward and energy-efficient process for producing cost-effective industrial-scale nanocellulose xerogels. However, further study are needed to improve the porosity and offer similar properties to aerogels achieved by supercritical drying.

3.2. Characterization of nanocelullose aerogels

Nanocellulose aerogels are nanostructured porous materials with outstanding properties stemming from their low density and extensive specific surface area. Appropriate characterization techniques are essential for understanding the influence of the different stages of synthesis on the final aerogel proprieties. By combining structural and physical analysis, it is possible to evaluate the structure-to-property relationship, therefore enabling the optimization of production processes while improving the final product's characteristics. In this section, we will provide a concise overview of the methods employed to assess the structural, morphological and mechanical properties of nanocellulosic aerogels.

3.2.1. Density and porosity

The final properties of nanocellulose-based aerogels are greatly governed by the density and the pore size. These attributes are significantly impacted by both the synthesis method and the processing pathway. For example, the pore size and distribution varies significantly according to the drying method. Quantitative and non-destructive diffusion techniques are used to investigate the aerogel skeleton and its connectivity.

3.2.1.1. Density measurement. A set of aerogel's properties, such as compressive strength and electrical conductivity, are dependent on the bulk density. Density measurement of aerogels can be divided into two physical parameters: the envelope density ρ_e and the skeletal density ρ_s (Reichenauer, 2011). The envelope density is applied for aerogels of regular shape such as cubes and cylinders. In this case, the volume can be estimated by dimensional analysis (i.e. measuring the dimensions of the aerogel with a compass) or by using the GeoPyc device. The mass is usually measured with a microbalance as most of aerogels are lightweight due to their very low density. Thus, ρ_e is expressed as the ratio of mass to volume of the material. On the other hand, the skeletal density corresponds to the total volume of nanoparticles composing the aerogel. In this case, an approximate volume can be obtained using a helium pycnometry technique (Ayral et al., 1992). Since helium has smallest atomic radius of any Earth's element, this monoatomic gas goes into all open pores without any interaction with the substrate. However, the impact of adsorbents present on the aerogel's surface may be neglected through this method. In the case of nanocellulose-based aerogel, a strong affinity exists between cellulose and hydroxylated systems, especially for small molecules such as water (Moon et al., 2011). Water aggregates adsorb onto the outer surface of the aerogel may affect the density measurement.

3.2.1.2. Nitrogen sorption. The structure of aerogels is governed by specific surface area and pore size distribution. Typically, nitrogen adsorption/desorption isotherms are employed for the purpose of conducting pore analysis (Scherer, 1998). The profile of the isotherm allow to draw quantitative information about the specific surface area and the pore size distribution for each porous sample. Gas sorption analysis investigates interactions between nitrogen gas and the adsorbent (Wang et al., 2016). These interactions take place when nitrogen is adsorbed within the microspores, forming mono- and multilayers on the inner surface of the aerogel. Adsorbed gases and vapor such as water molecules are removed from the sample by applying heat and vacuum prior to the measurement. Then, the aerogel is placed in a vacuum analysis tube and cooled to 77 K (liquid nitrogen N_2). Nitrogen gas is charged into the aerogel with controlled released. After each increment, the system reaches a stable state and the volume of adsorbed gas is measured. Equilibrium measurements are performed until adsorption ends and saturation pressure is reached. During the analysis an isotherm is plotted showing the specific amount adsorbed as a function of relative pressure (Nitrogen partial pressure over the saturation pressures). The low-pressure region corresponds to microspores adsorption, while the higher-pressure regions corresponds to mono- and multilayer adsorption (Horvat et al., 2022). Therefore, the surface area of the aerogel can be quantified by the Brunauer–Emmett–Teller (BET) equation that provides a theoretical relation between the volume of gas adsorbed and the volume of gas required to form a monolayer (Brunauer et al., 1938). Thus, the BET's surface area can be calculated using the adsorbed volume measurements in the monolayer segment. The pore size distribution of meso- and macroporous aerogels can be measured by applying the Barrett-Joyner-Halenda (BJH) model (Joyner et al., 1951). This approach is based on the kelvin-equation which relates the pore size to the pore condensation pressure. In the case of microporous aerogels, the pore size distribution is quantified by Density Functional Theory (DFT) method (Lastoskie et al., 1993).

3.2.2. Morphology

The evaluation of the pore morphology and the 3D structure of aerogels requires the synergy of several techniques. Scanning electron microscopy (SEM) and X-Ray tomography are techniques capable to provide quantitative informations on the shape and the porous morphology of aerogels.

3.2.2.1. Scanning electron microscopy. Nanocellulose-based aerogels are open mesoporous structures. Scanning electron microscopy (SEM) allows the investigation of pore shapes and aerogel interconnected structures. SEM images are produced by scanning the aerogel surface with a focused beam of electrons. These electrons interact with the material atoms, producing various signals bearing information about the surface topography (Pajonk et al., 1996). However, although the pores are clearly observable in the SEM images, the accurate measure of the pore size is often limited due to irregular pore shapes.

3.2.2.2. X-ray tomography. X-ray tomography is a non-destructive method employed for the 3D-visualization and characterization of matter, as shown in Fig. 4. This method exploits the penetrating power of X-rays to obtain a series of two-dimensional radiographs of the object recorded across different directions. From these 2D X-rays projections it is possible to stack transverse slices into a 3D assembly by using a reconstruction algorithm (Ganesan et al., 2016). X-ray tomography is a very powerful tool to visualize the three-dimensional, monolithic, and porous structure of aerogels.
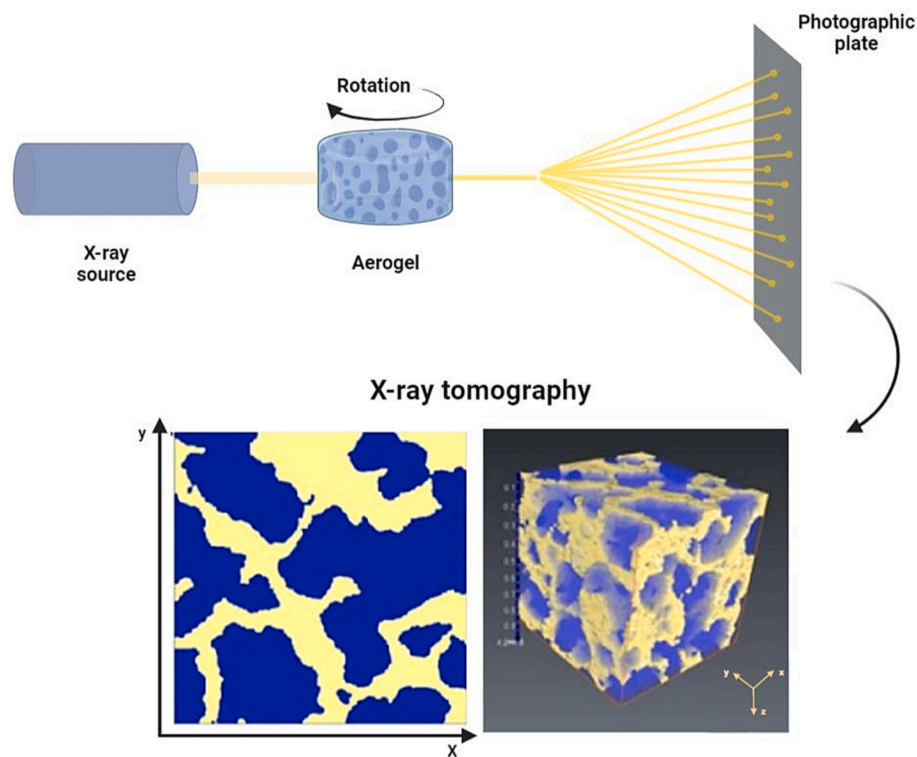
Fig. 4. Schematic representation of an X-ray assembly and a μ-computed X-ray tomography (μ-CT) image of calcium thiocyanate-stained cellulose aerogel. Adapted with permission from (Ganesan et al., 2016).

3.2.3. Mechanical characterization

To develop an aerogel for load-bearing uses, it is important that the material exhibit suitable mechanical properties. However, standards for mechanical tests specific to aerogels are not defined so far. The properties of nanocellulose-based aerogels are usually tested by uniaxial compression test (Zhou et al., 2019). This test quantify the recovery rate and the stress-strain curves across three distinct regions: i) the low-strain linear elasticity region where pore wall deformation occurs, ii) the plateau region of moderate strain where rapid pore collapse occurs, and iii) the high-strain densification region where collapsed pores begin to compress against each other resulting in hardening. Nanocellulose-based aerogels often exhibit good mechanical performance due to the inherent high strength of the cellulose nanofibers. In principle, aerogel's high mechanical strength is mainly due to its high density (Sehaqui et al., 2011).

3.2.4. Thermal conductivity

Aerogels are highly porous materials with very low thermal conductivity making them excellent candidates as thermal insulators. The thermal conductivity is usually measured in the in-stationary regime where the conductivity and the diffusivity are measured simultaneously (Illera et al., 2018). This measurement is performed either by hot wire or hot plate methods. In the hot wire method, a wire (usually made of platinum) is placed between two aerogel disks acting as a temperature sensor (Coquard et al., 2006). The wire is heated and the temperature is measured as a function of time. In the hot plate method, the material is placed between two plates: one of them is heated and the other one serves as a thermal sensor (Rottmann et al., 2020). The temperature increases and the heat flow is recorded on the control plate. In both approaches, the thermal conductivity is derived from the recorded thermograms. Nonetheless, as the thermal conductivity of aerogels is inherently low, the values acquired through both devices generally show variations and errors due to the imperfections of the assembly. Thus, the values of conductivity can vary up to 20 % for the same aerogel. Reducing the measurement error of aerogel thermal conductivity can be achieved by conducting measurements on various sections of the aerogel. Indeed, aerogels exhibit anisotropic properties, meaning that the porous structure and pore distribution may vary from one section to another, resulting in different thermal conductivities along different directions. Conducting measurements in multiple orientations and providing an average value, can enhances the reliability of the obtained thermal conductivity values.

3.2.5. Electrical conductivity

Nanocellulose-based aerogels are suitable for microwave-transmission systems stemming from their low electrical conductivity (Long et al., 2018). For energy storage devices, the incorporation of conductive materials such as carbon nanotubes is further required to improve the conductivity of nanocellulose aerogels (Pääkkö et al., 2008). Generally, electrical conductivity measurement is done by the four probe method (Shen et al., 2004). The measuring head is specially designed for low-resistance materials (conductors and semiconductors). The four probes are vertically arranged with equal spacing between each probe. A current flows through the outer pins, resulting in a measurable potential difference between the inner pins. This potential difference depends on the surface resistance of the aerogel and its structure.

4. Overview of the aerogels CO_2 adsorption mechanism

Aerogels exhibit versatile structural properties, making them as ideal candidates for a range of carbon capture applications (Keshavarz et al., 2021). Their porous structure offers a high specific surface area, which can promote interactions with CO_2 molecules. Manipulation of their distinct textural attributes is possible by modifying synthesis and processing conditions (Lavoine and Bergström, 2017). In addition, a thorough understanding of the adsorption mechanism, including kinetic and isothermal models, allows an assessment and optimization of CO_2 adsorption selectivity and efficiency.

4.1. CO_2 adsorption mechanism

Adsorption is a surface separation phenomenon that take place when a gas, a liquid, or a solid adheres to the surface of a material (adsorbent) (Kecili and Hussain, 2018). The adsorption process of CO_2 by an aerogel involve the interaction of gas molecules with the aerogel surface by physical forces or chemical bonds (Scherer, 1998). Physical adsorption occurs through weak Van der Waals interactions (Aljamali et al., 2021). Chemical adsorption takes place as valence electrons exchange between the atoms on the surface of the aerogel and CO_2 molecules to form a strong covalent bond (Sai Bhargava Reddy et al., 2021). In the adsorption process, the aerogel's properties such as the pore size, the polarity, and the surface structure; govern the type of interaction between the gas and the solid (Nakao et al., 2019). Therefore, the type, the synthesis, and the processing conditions of aerogels are the key points in CO_2 adsorption. Specifically, these adsorbents need to demonstrate high adsorption capacity, thermal stability, fast adsorption kinetic, gas selectivity, and easy regeneration. However, the interaction between CO_2 and the aerogel should not be too strong, as this may lead to an irreversible adsorption, and consequently single-use adsorbent.

4.1.1. Adsorption isotherms

Adsorption isotherms quantify the equilibrium-state interactions between adsorbates and adsorbents. These curves describe the amount of CO_2 adsorbed on the aerogel as function of the pressure at constant temperature. In general, the adsorption process involves a series of stages: (i) CO_2 molecules diffusing toward the surface; (ii) CO_2 diffusion into the pores of the aerogel; (iii) interaction with active sites; and (iv) the creation of an adsorbent layer on either the pore surface or walls (Nakao et al., 2019). Adsorption isotherms enable the prediction and the comparison of aerogels adsorption performance. These isotherms quantify the interactions of the CO_2 with the aerogel. The strength of the interaction is commonly indicated by the isosteric heat of CO_2 adsorption, which can be computed from CO_2 adsorption isotherms collected at varying temperatures through the utilization of the Clausius-Clapeyron equation (Keshavarz et al., 2021). Thus, by optimizing the aerogel's pore size and surface chemistry, the isosteric heat can be adjusted. Therefore, adsorption isotherms are essential to design effective adsorption systems. So far, 15 different isotherm models have been developed to study the adsorption behavior (Keller and Staudt, 2005). Among them, Langmuir, Freundlich, Dubinin-Radushkevich, Sip, Halsey Temkin, or Redlich-Peterson isotherm models are frequently used. The Langmuir model stands as the fundamental theoretical approach of isotherms (Eq. (2), Table 1). It is the most commonly used model for quantifying CO_2 adsorption on nanocellulose-based aerogels, followed by the Freundlich model (Eq. (3), Table 1) (Ho and Leo, 2021). The Langmuir model describes adsorption by the formation of an adsorbate monolayer on the aerogel's surface in which all sorption sites are identical. The isothermal Freundlich model relies on the heterogeneity and the multilayer adsorption mechanism. Generally, the adsorption takes place at sites with varying adsorption energies.

4.1.2. Adsorption kinetics

Quantification of the adsorption kinetics enables the prediction of the adsorption rate and the time required to reach the equilibrium state. The adsorption kinetic equation is assumed to follow the behavior of a heterogeneous chemical reaction at the gas-solid interface (Nakao et al., 2019). A plethora of adsorption kinetic models describing the operation of the adsorption process have been reported (Kecili and Hussain, 2018). These models describe the diffusion rates, the progression of the chemical interaction, and the mass transfer processes (Anas et al., 2017; Keshavarz et al., 2021). Pseudo-first order kinetic model is mainly used for adsorption processes governed by physisorption and controlled by surface diffusion (Eq. (4), Table 1). The pseudo-second order kinetic models based on the assumption that chemisorption is the rate-limiting step in the adsorption processes at the gas-solid interface (Eq. (5), Table 1). However, these models do not include the diffusion mechanism. Indeed, Romero et al. illustrate that in cases where adsorbed particles are sizable or the intrinsic reaction rate outpaces the diffusion rate of adsorbed species within pores, intra-particle diffusion constrains the adsorption rate (Guarín Romero et al., 2018). Consequently, alternative models have been designed to encompass several adsorption stages and include mutually surface and intra-pore diffusion (Martín et al., 2016).

4.2. Factors affecting the CO_2 adsorption

The capacity for adsorption is significantly controlled by the interactions between the aerogel and CO_2 molecules. These interactions are governed by several factors, such as the texture, the aerogel's surface chemistry, the moisture tolerance, the temperature, or the CO_2 flow pressure. Thus, the development of efficient CO_2 adsorbents requires a rational conception considering both thermodynamic and kinetic factors. In this section, we will highlight the factors that can improve the interactions and increase the rate of CO_2 adsorption.

4.2.1. Aerogels structure

The adsorption of CO_2 by aerogels occurs through Van der Waals forces, electrostatic interactions, and/or the establishment of chemical bonds. Previous studies have indicated that the CO_2 adsorption capacity of porous materials is contingent upon the existence of certain micropore structure (Querejeta et al., 2018). Generally, micropores can be categorized into ultramicropores (pore size <0.7 nm) and supermicropores (pore size ranging from 0.7 to 2.0 nm). The ubiquity of ultramicropores compared to larger pores significantly improves the CO_2 adsorption capacity (Yurduşen et al., 2020). Indeed, as the pore size decreases, the intermolecular force generated between adjacent walls intensifies. During the process of adsorption, the potential fields of these neighboring barriers intersect, thereby elevating the interaction energy between CO_2 and the adsorbent (Querejeta et al., 2018). Thus, theses stronger interactions lead to higher adsorption capacity. Nevertheless, aerogels based on nanocellulose feature a porous structure comprising a combination of meso- and macropores. Only a few studies have reported

Table 1
Isotherm models used for quantifying CO_2 adsorption on nanocellulose-based aerogels.

Model		Expression	Parameters		Eq. N°
Isotherm	Langmuir	$q_e = \dfrac{q_m\,K_L\,C_e}{1 + K_L\,C_e}$	q_e: amount of adsorbate in the adsorbent at equilibrium (mg·g^{-1})	K_L: Langmuir isotherm constant (L·mg^{-1}) q_m: maximum monolayer coverage capacities (mg·g^{-1})	(2)
	Freundlich	$q_e = K_f\,C_e^{1/n}$	C_e: equilibrium concentration (mg·L^{-1})	K_f: Freundlich isotherm constant related to adsorption capacity (mg·g^{-1}) (L·g^{-1})$^{1/n}$ n: Freundlich isotherm constant related to adsorption intensity	(3)
Kinetic	Pseudo-first order	$q = q_e\left(1 - e^{-tK_1}\right)$	q: adsorption per mass of adsorbent (mmol·g^{-1}) q_e: adsorption amount per unit mass of adsorbent at equilibrium (mmol·g^{-1})	K_1: pseudo-first order rate constant (min^{-1})	(4)
	Pseudo-second order	$q = \dfrac{q_e^2\,K_2 t}{1 + q_e K_2 t}$		K_2: pseudo-second order rate constant (mmol·g^{-1}·min^{-1})	(5)

the effect of the pore size and the specific surface area on the adsorption capacity of mesoporous sorbents such as nanocellulose-based aerogels. However, Chen et al. have studied the effect of the pore size on CO_2 adsorption capacity of tetraethylenepent-amine/carbon aerogels (Chen et al., 2019). This study come to the conclusion that enhancing pore size enhances adsorption kinetics, as higher pore volume facilitates the efficient transport of gas molecules into the aerogel pores. As regards to the effect of the specific surface area, it is generally assumed that a higher pore number is favorable to CO_2 mass transfer. Anas et al. quantified the CO_2 absorption performance of various aerogel types as a function of their specific surface area, pore diameter, and pore volume (Anas et al., 2017). The goal of the study was to evaluate the relationship between CO_2 physisorption and textural properties. Outcome of the study revealed that CO_2 adsorption correlated well with the increase of the mesoporous area of each aerogel. It is clear from these studies that the capture capacity does not only depend on the pore size distribution but also on the specific surface area and the total pore volume.

4.2.2. Surface functionalization effect

The Aerogel/CO_2 interactions also plays a pivotal role in influencing the adsorption capacity. Enhanced interactions can be achieved by functionalizing the pore surface to improve affinity with CO_2 molecules. The mechanism of CO_2 adsorption on the amine-functionalized aerogel is illustrated in Fig. 5. CO_2 is a weak Lewis acid containing an empty orbital capable of accepting a pair of electrons from a Lewis base. The nitrogen atom can act as a Lewis base by contributing its unpaired pair of electrons (Said et al., 2020). Thus, the grafting of amine group on the aerogel surface generates quadrupole moment interactions between the CO_2 molecules and the polar nitrogen element, resulting in an increased adsorption capacity. The surface functionalization can be prepared by one-pot approaches or post-synthetic methods (Kong et al., 2014). The later technique consists in the preparation of the aerogel followed by the surface functionalization. The post-synthetic technique is commonly used, as it allows easy control of the substrate's textural properties (Wörmeyer et al., 2012). The type of amine can also strongly influence the CO_2 capture efficiency of the modified aerogels. Thus, a high amine loading is favorable to a high adsorption capacity. Linneen et al. evaluated the CO_2 adsorption capacity of aerogels grafted with mono-, di- and tri-amino silanes (Linneen et al., 2014). It was shown that as the number of amine units per silane increases (i.e. tri > di > mono), the quantity of grafted nitrogen increases, and consequently the CO_2 adsorption capacity increases. However, overloading the aerogel with amine can lead to aerogel shrinkage, destroy the pore structure and block the network between the pores (Linneen, 2014).

4.2.3. Humidity effect

Humidity can also affect the CO_2 adsorption capacity of aerogels. During adsorption in humid conditions, CO_2 molecules can link with amine groups to produce carbamates intermediates (Yu et al., 2018). The reaction mechanism differs from the type of amine groups, the amine charge, and the moisture content. Several studies revealed that moisture influence the adsorption capacity of CO_2 (Zhang et al., 2017). In dry conditions, a pair of amine moles react with one CO_2 mole, forming alkylammonium carbamate zwitterions. In the presence of moisture, two possible side-reaction occurs leading to bicarbonate or carbamic acid functionalities. Therefore, complexation improves the amine's efficiency with a stoichiometric ratio of 1:1 between amine and CO_2 (Said et al., 2020). In addition, the co-adsorption of some water present in the gas stream lead to an increase of the sorbent stability. In fact, the water will inhibit the formation of unwanted urea during the regeneration process (Kong et al., 2014). However, excessive moisture content can induce adverse changes in the microstructure of the adsorbent (pore clogging), or severely affect the energy requirement at the regeneration process to remove the adsorbed water.

4.2.4. Temperature effect

The temperature has a noteworthy effect on the adsorption kinetics. Raising the reaction medium's temperature should result in the increase of the average rate of the gas particles. Then, the increase of the average velocity would therefore lead to an increase of the kinetic energy of the system, and thus increase the adsorption capacity (Anas et al., 2017). However, some researchers have shown that the quantity of adsorbed CO_2 declines with increasing temperature (Marques et al., 2016). This tendency could be explained by the decrease of covalent interactions between amine groups and CO_2 at high temperature. To prevent this trend, it is possible to predict the optimal adsorption temperature from adsorption isotherms at different temperatures. In general, the transition from the gas to the adsorbed state, so called adsorption, is an exothermic process. With respect to Le Chatelier's principle, the quantity adsorbed at the equilibrium state must therefore be compensated either by the decrease of the temperature or by the increase of the pressure. Indeed, an exothermic reaction must be attenuated by an endothermic mechanism. However, lower temperature of adsorption can also slow down the mass transfer and thus decrease the adsorption capacity of the system (Kong et al., 2014). Therefore, the most optimal temperature range for the adsorption system must be carefully defined.

4.2.5. Pressure effect

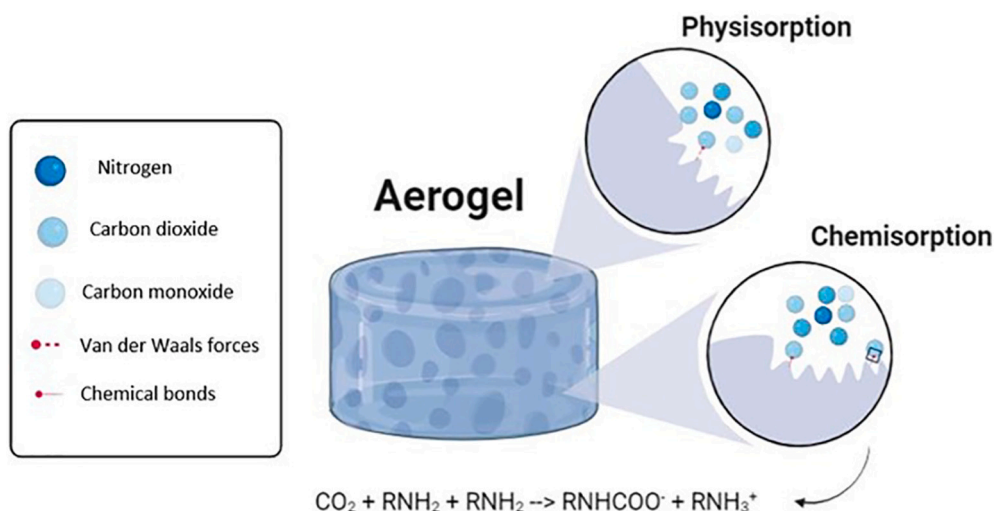Numerous studies have reported an increase in the adsorption

Fig. 5. Diagram illustrating the physisorption and chemisorption processes of CO_2 adsorption on aerogels.

capacity of aerogels with rising pressure (Anas et al., 2017). The global volume of the adsorbent decreased when a gas is adsorbed on surface. Thus, based on Le Chatelier's principle, the application of a stress (such as a change in pressure) on a system will shift the equilibrium state toward a new state that will counteract the applied stress. To face the increase in pressure, the system will tend to reduce the number of molecules in the gas phase, thereby increasing the adsorption capacity of CO_2 on the adsorbent surface. Other parameters that may influence the adsorption capacity such as contact time or CO_2 concentration have been barely investigated (Kong et al., 2016).

5. CO_2 adsorption using nanocelluose aerogels

Nanocellulose aerogels have several outstanding attributes including good mechanical properties, low density, and high specific surface area fully accessible to gas capture. Their adaptability is particularly noteworthy in tasks involving the adsorption and separation of CO_2 in mixed gases (Zhu et al., 2024), as well as their use as effective air filters (Sepahvand et al., 2023). However, pure nanocellulose has poor affinity for CO_2 molecules (Zhang et al., 2019). The sorbent-sorbate affinity is a critical factor for the adsorption capacity. Improving these affinities is important to produce a nanocellulose-based aerogels with an efficient CO_2 adsorption capacity. For this purpose, Wei et al. developed CO_2 adsorbents based on freeze-molded CNFs aerogels impregnated with acetylated CNCs fixed via a capillary force process (Wei et al., 2020). The modified CNCs with acetyl groups on the surface contribute to a better CO_2 affinity. In fact, the addition of oxygen molecules provides an attractive and rich electron site favorable to CO_2 binding (Fig. 6). Functionalized aerogels exhibit improved mechanical performance and a better CO_2 adsorption (1.4 mmol·g^{-1}). Another technique to improve CO_2/aerogel interactions is to develop high performance carbon adsorbents produced from lignocellulosic biomass. Recently, Geng et al. have successfully developed biobased aerogels from lignin and cellulose nanofibers (CNFs) materials (Geng et al., 2021). The resulting adsorbents demonstrate great potential for the CO_2 capture. Lignin, which is

the main component conferring the rigidity and strength to plant cell walls, has a high content of aromatics and hydroxyl groups beneficial for CO_2 adsorption processes. The derived monolithic organic aerogels show a hierarchical porous structure with homogeneous macrospores favorable to a fast adsorption kinetic (Fig. 6). The final pore structure and properties varied with the lignin/CNFs ratio, the solids content of the starting suspension, and the carbonization time. The monolithic carbon adsorbent developed from a 85:15 lignin:CNFs ratio carbonized during 1 h exhibit efficient CO_2 adsorption capacity (4.49 mmol·g^{-1}), in a similar range than carbonaceous adsorbents synthesized via complex procedures.

Innovative pathways have been explored to enhance the CO_2 adsorption capacity by functionalizing nanocellulose aerogels using amine groups or by incorporating materials known for large adsorption capacity. In the following section, the progress achieved to increase the adsorption capacity of nanocellulosic aerogels, from functionalization to composite development, will be discussed.

5.1. Functionalization of nanocellulose aerogels for CO_2 adsorption

The hydroxyl-rich nanocellulose surface can be grafted with a myriad of aminosilane groups. The surface functionalization can be induced by gas or aqueous phase methods. Various techniques for the amine functionalization of aerogels are reported in Table 2. N-(2-aminoethyl)-3-aminopropylmethyldimethoxysilane (AEAPMDS) was used to modify cellulose nanocrystal extracted from poplar residue (Wu et al., 2017). The modification was performed in aqueous phase under ultrasound irradiation. The aerogel was obtained by supercritical drying. The AEAPMDS-based CNCs aerogel exhibits a BET surface area of 287 m^2·g^{-1}, allowing CO_2 adsorption up to 2.6 mmol·g^{-1} at 273 K. Similarly, AEAPMDS was grafted onto a spherical CNCs hydrogel using an aqueous phase heat treatment (Zhang et al., 2019). The aerogel was produced by a tert-butanol solvent exchange and freeze-drying. The resulting porous materials present a lower specific surface area (77 m^2·g^{-1}) as compared to the CNCs aerogel prepared by supercritical drying. The lower specific
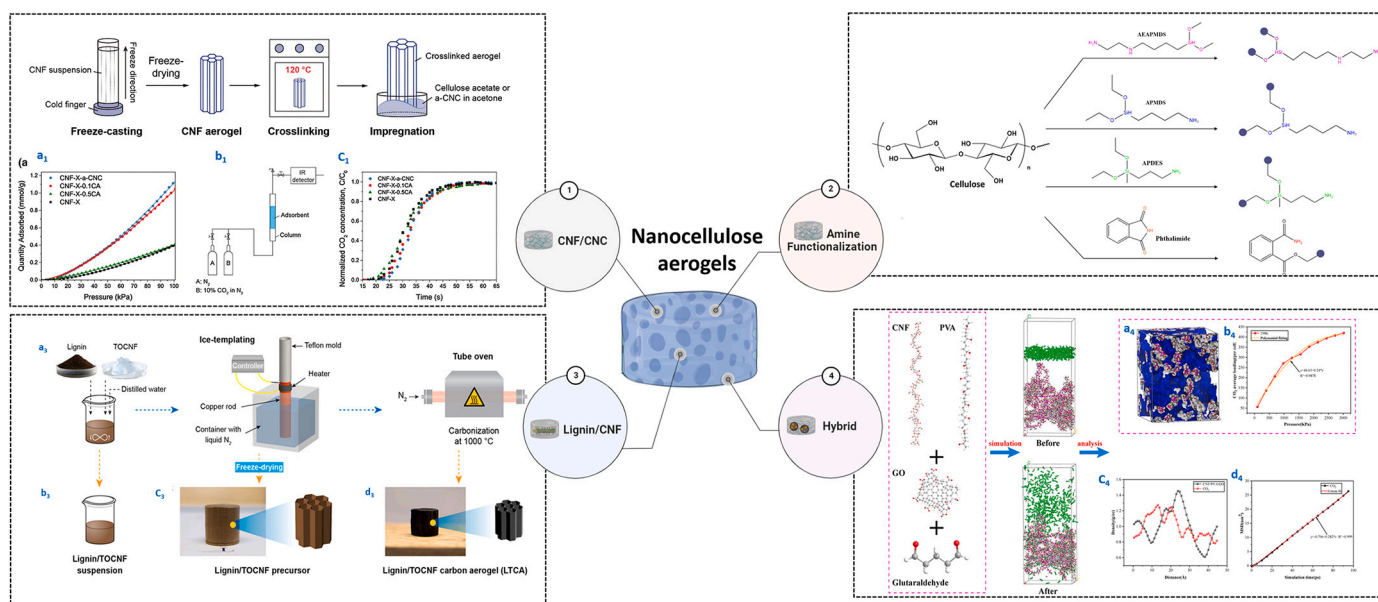

Fig. 6. Illustration of the synthesis procedure for nanocellulose aerogels as CO_2 adsorbents: 1) CNFs aerogel impregnated with acetylated CNCs: a$_1$) Adsorption isotherms of the CNF-X-a-CNC aerogel, b$_1$) Schematic illustration of CO_2 breakthrough equipment, c$_1$) Graphs illustrating breakthrough curves of CNF-X-a-CNC aerogel. Reproduced from (Wei et al., 2020) with permission, 2) Functionalization reactions of cellulose with amines for enhanced CO_2 adsorption. 3) a$_3$) Production process and illustrations of lignin/CNF aerogel, including, b$_3$) lignin/TOCNF suspensions, c$_3$) lignin/TOCNF precursors, and d$_2$) LTCAs. Reproduced from (Geng et al., 2021) with permission, 4) Modelled molecular dynamics configurations of CO_2 adsorption onto CNF/PVA/GO aerogel: a$_4$) representation of aerogel's available volume, b$_4$) Monte Carlo simulation (sorption module) determining molecule count in the system, c$_4$) graph depicting relative motion between aerogel and CO_2, and d$_4$) diffusion curve illustrating CO_2 movement within aerogel. Reproduced from (Zhang et al., 2022) with permission.

Table 2
Summary of nanocellulose aerogel and their CO_2 capture capacity.

Support	Dried method	Amine functionalization	Functionalization method	S_{BET}[a] $(m^2 \cdot g^{-1})$	V_{total}[b] $(Cm^3 \cdot g^{-1})$	T[c] $(°C)$	P[d] (bar)	Adsorption capacity $(mmol \cdot g^{-1})$	Ref
CNFs/ CNCs	Freeze-drying	–	CNCs acetylated	21.04	–	0	1	1.14	(Wei et al., 2020)
Lignin/ CNFs	Freeze-drying	–	–	126	–	25	1	4.49	(Geng et al., 2021)
CNCs	Supercritical-drying	AEAPMDS	Liquid-phase	287.33	0.43	0	1	2.6	(Wu et al., 2017)
						25	1	1.7	
CNCs	Freeze-drying	AEAPMDS	Liquid-phase	77	0.60	25	3	1.68	(Zhang et al., 2019)
CNCs	Freeze-drying	AEAPMDS	Gas-phase	110.4	0.82	25	1	1.59	(Zhang et al., 2020)
CNCs	Freeze-drying	AEAPMDS	Gas-phase	29.14	0.15	25	1	1.50	(Zhu et al., 2020)
CNCs	Freeze-drying	APMDS	Gas-phase	95.2	0.41	25	11	2.57	(Xu et al., 2021)
CNCs	Supercritical-drying Freeze-drying	APMDS	Gas-phase	150.7 66.3	0.64 0.38	25	1	2.50 2.45	(Jia et al., 2022)
CNFs	Freeze-drying	APDES	Liquid-phase	7.5	–	25	1	2.3	(Gebald et al., 2014)
CNFs	Freeze-drying	AEAPMDS	Liquid-phase	7.1	–	25	1	1.39	(Gebald et al., 2011)
CNFs	Freeze-drying	AEAPMDS	Liquid-phase	36.4	0.177	20	1.35	1.78	(Liu et al., 2018)
CNFs	Freeze-drying	AEAPMDS	Liquid-phase	51.8	0.19	25	1	1.91	(Wu et al., 2018)
CNFs	Freeze-drying	APMDS	Liquid-phase	59.2	0.22	0	1	2.4	(Li et al., 2020)
CNFs	Freeze-drying	Phthalimide	Liquid-phase	335	60.3	25	0.2	5.2	(Sepahvand et al., 2020)

[a] BET surface area.
[b] Pore volume.
[c] Temperature.
[d] Pressure.

surface area results from the pore shrinking which prevents the structural stability of the aerogel. Thus, the CO_2 adsorption capacity reaches 1.68 $mmol \cdot g^{-1}$ under normal temperature and pressure conditions. The improved adsorption capacity of APEDMS-functionalized nanocellulose aerogel inspired Zhang et al. to graft aminosilane functions onto CNCs by a gas-phase modification method (Zhang et al., 2020). The ultrasonically dispersed CNCs suspension was dropped in $CaCl_2$ solution, and the resulting spherical wet gel was replaced by tert-butyl alcohol and finally dried using freeze-dryer technique. Then, functionalized CNCs aerogel was obtained through APEDMS gas-phase grafting. Usually, the aminosilane is dissolved in the solvent in the aqueous-phase method (Zhang et al., 2019). This dissolution favors its self-condensation resulting in high consumption of aminosilane and low modification rate. Therefore, using chemical vapor deposition to obtain aminosilane-based CNCs aerogel not only improve the efficiency of the chemical modification, but also provide higher CO_2 adsorption capacity. Consequently, the resulting CNCs aerogel achieved a significantly improved CO_2 adsorption capacity, reaching 1.59 $mmol \cdot g^{-1}$, 7 times higher than the unmodified aerogel (0.19 $mmol \cdot g^{-1}$). However, this absorption rate remains in the same range than AEAPMDS-grafted aerogels using the aqueous phase route. This slightly lower adsorption capacity may originate from the pore clogging which results in a reduction of the specific surface area by almost 50 %. To overcome this effect, Xu et al. modified CNCs using an aminosilane of intermediate chain length (Xu et al., 2021). The CNCs suspension was ultrasonicated to form a uniform CNCs colloid. CNCs wet gel beads were prepared and then gelled in an aqueous $CaCl_2$ solution. Subsequently, the cellulose nanocrystal hydrogel beads underwent a series of steps involving solvent exchange to attain the alcogel state, followed by freeze-drying. The CNCs aerogel was finally functionalized using 3-aminopropyl-methyl diethoxysilane (APMDS) via a vapor phase reaction. Pretreatment with triethylamine has proved to significantly improve the functionalization efficiency and reduce the temperature of the grafting reaction. The amine loading of the CNCs aerogel was up to 7.06 $mmol \cdot g^{-1}$. Chemical adsorption significantly dominated on the CNCs aerogel with a total adsorption capacity of 2.57 $mmol \cdot g^{-1}$ (room temperature, $P = 101.33$ kPa), higher than previously reported nanocellulose-based adsorbent. Later, Jia et al. studied the effect of aerogel synthesis methods on the functionalization and adsorption rate (Jia et al., 2022). CNCs aerogels produced by freeze-drying and

CO_2 supercritical drying were coated with APMDS by a vapor phase reaction. The grafting occurred only on the CNCs surfaces resulting in a similar amine loading on the two pristine CNCs aerogels (about 7.2 $mmol \cdot g^{-1}$). The CNCs aerogel formed by CO_2 Sc-drying had a higher BET's specific surface area (S_{BET}) and pore volume size than the CNCs aerogel dried using freeze-drier. Following the modification, there was a noticeable decrease in the microstructure parameters of the aerogels. These changes were attributed to the pore blocking by the grafted APMDS. At low pressures, CNCs-Sc-CO_2 aerogel showed slightly higher CO_2 adsorption than CNCs-FD, probably due to the higher specific surface area. At higher pressures, chemical adsorption by the introduced amine groups was predominant over physical adsorption. The total CO_2 uptakes for both modified aerogels reached 2.5 $mmol \cdot g^{-1}$ (room temperature, $P = 100$ kPa).

Using similar strategies, cellulose nanofibers (CNFs) have been successfully modified to develop high performance CO_2 adsorbents. Compared to CNCs aerogels, CNFs aerogels exhibit uniform pore size distribution, better thermal stability, and superior physical and mechanical properties (Zhu et al., 2021). Gebal et al. have developed CNFs-based aerogels obtained by a two-step mechanical isolation process (Gebald et al., 2014). The CNFs were functionalized with 3-aminopropylmethyldiethoxysilane (APDES). The suspension of aminosilane-modified nanofibers was then poured in liquid N_2 and freeze-dried. The nitrogen content and S_{BET} of APDES-CNF were measured at 4.2 $mmol \cdot g^{-1}$ and 7.5 $m^2 \cdot g^{-1}$, respectively. Despite the relatively low specific surface area, the increased loading of functional groups of APDES-CNFs enable a CO_2 adsorption capacity of 1.1 $mmol \cdot g^{-1}$ (room temperature, $P = 0.04$ kPa). At higher pressures, a maximum of the CO_2 adsorption was observed, reaching up to 2.3 $mmol \cdot g^{-1}$ at 100 kPa. In comparison to the CO_2 adsorption performed under dry conditions, moisture slightly enhances the capture efficiency. To quantify moisture impact on adsorption capacity of amine-functionalized aerogels, the same research team developed adsorbents synthesized from the freeze-drying of an aqueous suspension of nanofibrillated cellulose (NFC) and AEAPDMS (Gebald et al., 2011). The CO_2 absorption rate was measured using wet air adsorption at 40 % relative humidity. The amine functionalization drastically reduced the S_{BET} from 26.8 to 7.1 $m^2 \cdot g^{-1}$ for the native and modified aerogel, respectively. However, even if the S_{BET} is relatively low as compared to other systems, the CO_2 capture

reach 1.39 mmol·g^{-1} for the functionalized aerogel, a value slightly higher than the dry flow adsorption. To improve the S_{BET}, Liu et al. developed functionalized, ultralight, and spherical aerogels by a suspension titration method using an efficient amination process (Liu et al., 2018). CNFs were firstly extracted from eucalyptus pulp, then formulated by ultrasonication method, and subsequently gelified using a CaCl$_2$ solution. Spherical CNFs-hydrogels were then introduced into an aqueous solution of AEAPMDS with different mass fraction. Following the chemical grafting, the spherical aerogels were finally obtained by solvent exchange with tert-butanol and freeze-drying technique. Amino-modified spherical CNFs-based aerogels exhibited outstanding thermal stability and high nitrogen content (5.4 %). The aerogel displays larger specific surface area ($S_{BET} = 36.4$ m^2·g^{-1}) and enhanced CO$_2$ absorption capacity (up to 1.78 mmol·g^{-1}). Li et al. have described the impact of the reaction parameters on the amine loading while functionalizing CNFs with N-(2-aminoethyl)-3-aminopropylmethyldimethoxysilane (APMDS) (Li et al., 2020). CNFs were dispersed and subjected to functionalization with APMDS in various environmentally-friendly solvents. Then, amine-functionalized colloidal CNFs gel was immersed in liquid N$_2$ and freeze-dried. The effects of the main reaction parameters including APMDS mass fraction, reaction time, temperature, and stirring rate on the amine loading were studied during CNFs functionalization. The highest amine loading was obtained when TBA has been used as reaction medium ($N = $ 4.57, 6.49 and 7.69 mmol·g^{-1} for H$_2$O, EtOH and TBA, respectively). The high polarity of ethanol and water may result in hydrogen bonding with APMDS preventing functionalization onto the nanocellulose surface. The optimum reaction time and temperature allowing to reach a maximum amine loading of 9.05 mmol·g^{-1} were 4 h and 90 °C, respectively. At lower temperatures, aminosilanes tend to hydrolyse into aminosilanol which inhibits CNFs functionalization. The amine-loading was also found to increase with higher amounts of aminosilane (optimal amine-loading obtained using 6 % of APMDS). However, when the amount exceeds the threshold value of 6 %, the aminosilane functionalized onto the CNF's surface could cause steric hindrance, resulting in a decrease in the reaction rate. The functionalized CNFs aerogel exhibits a S_{BET} and pore volume of 59.2 m^2·g^{-1} and 0.22 cm^3·g^{-1}, respectively. The CO$_2$ adsorption capacity reaches 2.4 mmol·g^{-1} for this amine-functionalized aerogel. More recently, Sepah et al. have developed a promising process considering phthalamide to functionalize CNF's surface (Sepahvand et al., 2020). CNFs were extracted from Kraft birch pulp, modified using phthalamide, and finally freeze-dried. BET analysis revealed an increase in surface area and decrease in pore size after CNFs modification (Fig. 6). As the phthalimide concentration increased, the structure became denser and more compact, resulting in an increased density and a decreased porosity. Following the functionalization, the adsorption capacity increased from 2.2 mmol·g^{-1} for the pristine CNFs to a maximum CO$_2$ adsorption of 5.2 mmol·g^{-1} for the phthalamide-functionalized CNFs-based aerogel (1.5 % phthalimide dosage).

5.2. Hybrid nanocellulose aerogel for CO$_2$ adsorption

Hybrid materials are formed by combining the physical, chemical and mechanical properties of different compounds to enhance the performance of the adsorbent. These materials take advantage of the properties of different compounds in a single adsorbent, offering a high capture capacity stemming from a larger number of accessible adsorption sites. In recent years, several works focus on the development of hybrid nanocellulose aerogels combining renewable sources, biodegradability, and high adsorption capacity (Table 3). Jiang et al. synthesized a hybrid CNFs-silica aerogel via a sol-gel process using 2,2,6,6-Tetramethylpiperidinyloxy (TEMPO) oxidized CNFs and aqueous sodium silicate as precursors (Jiang et al., 2018). Hydrogels with homogeneously dispersed silica and CNFs were later functionalized using (3-Aminopropyl)triethoxysilane (APTES). The amine functionalized alcogel was then subjected to a solvent exchange with tert-butanol and freeze-dried into a hierarchical *meso*porous aerogel. This hybrid material exhibits an ultra-low density of 7.7 mg·cm^{-3}, a S_{BET} of 11 m^2·g^{-1}, and a pore volume of 0.02 cm^3·g^{-1}. An improvement of the mechanical properties was provided by the CNFs which acts as the structural backbone. On the other hand, increasing the silica content improves the thermal stability and allows CO$_2$ adsorption of 1.49 mmol·g^{-1}. Later, further development were conducted onto multicomponent hybrid aerogels with improved performance and multiple functions. Valence et al. developed a hybrid multicomponent aerogel based on metal-organic frameworks (MOFs), nanocellulose, and gelatin (Valencia and Abdelhamid, 2019). MOFs are highly porous compounds composed by metal ions coordinated to organic ligands, forming one-, two- or three-dimensional structures. The hybrid materials were designed by i) in situ synthesis of zeolitic imidazolate (ZIF-L) in nanocellulose at room temperature using water as green solvent, ii) incorporation of gelatin matrix, and iii) freeze-drying. This hybrid material was characterized by a hierarchical porous structure containing mesopores and macropores, providing a specific surface area of 10 m^2·g^{-1} and an ultra-low density of 37.4 kg·m^{-3}. The TOCNF/ZIF-L/gelatin aerogel displays a CO$_2$ adsorption capacity of 0.66 mmol·g^{-1}, enhanced by the amine groups present in the gelatin and by the cushion-shaped cavities of the ZIF-L. Using the synergy of the gelatin/nanocellulose network, Valence et al. developed hybrid foams based on gelatin and nanocellulose (Valencia et al., 2019). These original hybrid aerogels were developed to support ultra-high loads of colloidal zeolite silicalite-1, used here as a model sorbent nanomaterial. Zeolites are minerals formed by a crystalline microporous aluminosilicate skeleton with a 3D structure connected via oxygen bridges. The resulting porous material allow the capture of small molecules. These compounds exhibit significant potential as effective adsorbents for atmospheric CO$_2$, contributing to the ongoing efforts to combat climate changes. This hybrid aerogel combined zeolite micropores with meso/macropore of the biopolymer substrate offering an excellent diffusion of adsorbate gas molecules. Adsorption isotherms demonstrated an enhanced CO$_2$ adsorption capacity with increasing

Table 3
Summary of CO$_2$ capture of hybrid nanocellulose aerogels.

Support	Dried method	S_{BET}[a] (m^2·g^{-1})	V_{total}[b] (cm^3·g^{-1})	T[c] (°C)	P[d] (bar)	Adsorption capacity (mmol·g^{-1})	Ref
CNFs/silica	Freeze-drying	11	0.02	25	1	1.49	(Jiang et al., 2018)
TOCNFs/ZIF-L/gelatin	Freeze-drying	10	–	25	1	0.66	(Valencia and Abdelhamid, 2019)
TOCNFs/gelatin/Zeolite	Freeze-drying	250	1.9	25	1	1.30	(Valencia et al., 2019)
CNFs/PVA/GO	Freeze-drying	69.27	0.28	25	1	0.22	(Zhang et al., 2022)
CNFs/PVA/GO	Freeze-drying + carbonization	392.4	0.84	25	1	19.32	(Zhang et al., 2022)
TOCNFs/KGM/HKUST-1	Freeze-drying	688.5	0.29	25	1	3.50	(Sun et al., 2022)
CNFs-nZIF-8	Freeze-drying	95.2	–	25	5	3.90	(Rostami et al., 2022)

[a] BET surface area.
[b] Pore volume.
[c] Temperature.
[d] Pressure.

silicalite-1 content, confirming that the porous gelatin/nanocellulose support does not obstruct the zeolite pores or restrict the diffusion of gas molecules. Consequently, the presence of silicalite-1 leading to a substantial rise in the porosity and in the specific surface area of the foams. This structural modifications hold a notable influence on the adsorption capacity of CO_2 molecules, reaching a value of 1.3 mmol·g^{-1}. Another study reports the combination of graphene oxide (GO) with different matrix to produce high performance aerogels (Zhang et al., 2022). A CNFs/PVA/GO gel was prepared using a stepwise heating process that induce interaction forces between the polymer chains of poly(vinyl alcohol) (PVA) and CNFs-GO mixture (Fig. 6). Subsequently, a light and layered porous CNFs/PVA/GO carbon aerogel composite was prepared by freeze-drying, followed by carbonization to assess its impact on CO_2 adsorption efficiency. The carbonization process consists in pyrolyzing the aerogel under an inert gas atmosphere at temperatures above 600 °C. The resulting material consists in a highly porous carbon network with interconnected clusters of carbon nanoparticles with diameter ranging between 3 and 20 nm. The CNFs/PVA/GO aerogel composite showed a S_{BET} and a pore volume of 69.27 m^2·g^{-1} and 0.28 cm^3·g^{-1}, respectively. After calcination, the significant increase of the S_{BET} (392.41 m^2·g^{-1}) is attributed to the decomposition of soft segments. These new adsorbents exhibit a higher CO_2 capture capacity reaching 19.32 mmol·g^{-1}. In a green perspective, Sun et al. have developed a sustainable strategy to manufacture a nanofiber/konjac glucomannan (TOCNFs/KGM) aerogel vacuum impregnated with HKUST-1 metal-organic crystals (Sun et al., 2022). Combining MOFs with biomass aerogels has proven to be a successful method to develop a hybrid aerogel with a hierarchical pore structure offering numerous adsorption sites. The hybrid aerogel exhibits a high mechanical strength owing to the large number of hydrogen bonds formed by the TOCNFs/KGM cross-linking. The

combination of meso/macropores from TOCNFs/KGM biopolymer network and the microspores of HKUST-1 provides a large contact area enabling a notable CO_2 adsorption capacity up to 3.50 mmol·g^{-1} (room temperature, $P = 1$ bar). More recently, nanoMOFs were combined with CNFs to produce robust aerogels with excellent gas-absorbing properties (Rostami et al., 2022). These hybrid aerogels were prepared by mixing a dispersion of nanosized ZIF-8 MOF particles (prepared from the self-assembly of 2-MiM and Zn^{2+} ions), in a CNFs gel. The resulting aerogels fully exploit the intrinsic properties of the mechanically robust, the flexible CNFs network, and the high specific surface area of nanoMOFs (1470 m^2·g^{-1}). Finally, the combination of these outstanding properties allow a strong interfacial adhesion and great CO_2 adsorption capacity of 3.9 mmol·g^{-1}.

6. Approaches to enhance CO_2 adsorption capacity in nanocellulose aerogels

Considering all the valuable results mentioned above it is crucial to highlight that the advancement of nanocellulose aerogels with a high adsorption capacity involves the consideration of various factors. In the pursuit of optimizing CO_2 adsorption performance, one must carefully examine the synthesis and functionalization techniques employed. Fig. 7 presents a comparative map illustrating the impact of various factors on the CO_2 adsorption efficiency of nanocellulose aerogels.

The choice of drying methods, such as air drying, freeze drying, and supercritical drying, plays a pivotal role in determining the final properties of the nanocellulose hydrogel. Each drying strategy has distinct effects on the structure, porosity, and surface area of the aerogel, consequently influencing its adsorption capabilities. Indeed, air-drying, while simple and cost-effective, tends to generate nanocellulose
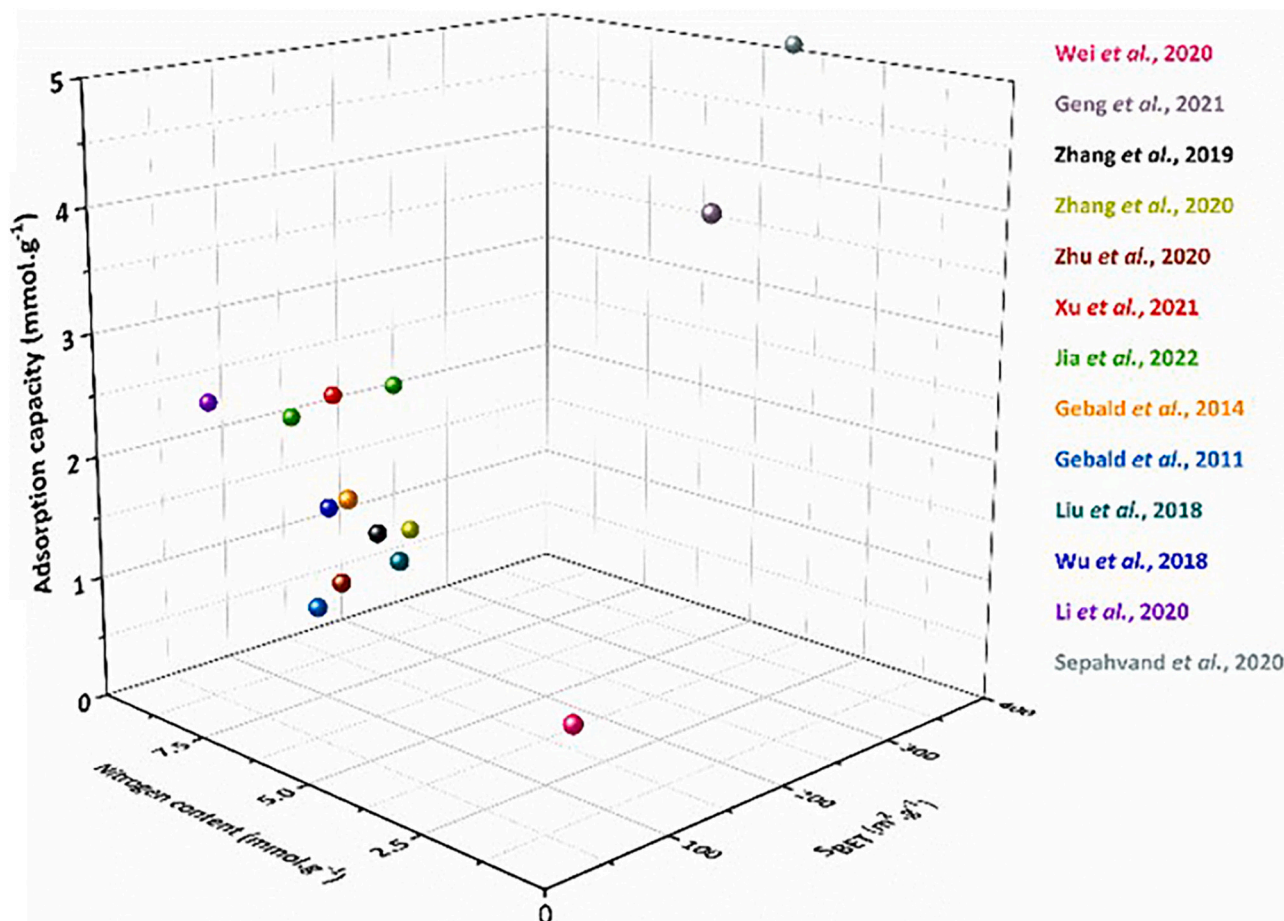

Fig. 7. Comparative map illustrating the impact of the surface area (S_{BET}) and nitrogen content on the CO_2 adsorption efficiency of nanocellulose aerogels.

hydrogels with low porosity, increased shrinkage, and structural defects. These results are largely attributable to strong hydrogen bonds. Only surface hydrophobization could preserve the porous structure of nanocellulose aerogels. In contrast, freeze-drying, renowned for its ability to maintain the porous structure, gives rise to hydrogels with increased porosity, improved mechanical strength, and more effective preservation of the nanocellulose network. As an advanced technique, supercritical drying outperforms others in terms of speed and efficiency, resulting in aerogels with exceptional porosity and superior mechanical properties. However, it requires specialized equipment and expertise. In general, the choice of drying method has a significant influence on the properties of nanocellulose hydrogels, with porosity ranking in the order: supercritical drying > freeze-drying > air-drying. Notably, starting with the same type of nanocellulose, drying with two different methods generates nanocellulose aerogels with a specific surface area of 287.33 m^2/g with supercritical drying (Wu et al., 2017), compared with 77 m^2/g with freeze-drying (Zhang et al., 2019).

The specific surface area of an aerogel has a significant influence on its CO_2 adsorption capacity. In theory, a larger surface area offers more active sites and increased exposure, thus favouring adsorption of a greater number of CO_2 molecules. The porous structure of aerogels, combined with a larger surface area, would normally improve overall adsorption efficiency. However, studies such as those carried out by Jia et al., 2022, comparing two aerogels dried using different methods, demonstrate that despite a larger specific surface area provided by supercritical drying, adsorption rates may remain equivalent. This may be explained by considerations related to pore size, as indicated by previous research (Anas et al., 2017; Chen et al., 2019). The CO_2 adsorption capacity of porous materials is closely linked to pore size. The abundance of mesopores, compared to larger pores, plays a crucial role in significantly improving CO_2 adsorption capacity. Reducing pore size intensifies the intermolecular force between adjacent pores walls, thereby promoting the adsorption of CO_2 molecules. However, it is generally assumed that the presence of macropores is favorable for the mass transfer of CO_2, acting as tunnels to guide CO_2 molecules toward mesopores. So, while specific surface area is an important parameter, other structural features, such as pore distribution, also influence CO_2 adsorption capacity. A thorough understanding of these complex interactions is essential to design optimized nanocellulose aerogels for improved adsorption performance.

Surface functionalization of nanocellulose aerogels is also a crucial parameter, having a significant impact on their CO_2 adsorption capacity. The introduction of amine groups on the aerogel surface creates additional interaction sites for CO_2 molecules. However, the method of modification and the type of amine used can significantly influence the adsorption rate. In the case of gas-phase surface modification, the more homogeneous distribution of amine groups improves the distribution and accessibility of these active sites, resulting in a higher adsorption rate (Zhang et al., 2019). On the other hand, liquid-phase modification led to less uniform functionalization, resulting in blocked pores, decrease of surface area, and inhibited adsorption of CO_2 molecules (Wu et al., 2017). The molar ratio of amine introduced can also significantly influence the CO_2 capture efficiency of modified nanocellulose aerogels. A high concentration of amine promotes a high adsorption capacity. However, an excessive amine load can lead to the shrinkage of the aerogel, damage the pore structure, and obstruct connectivity between pores. For instance, using the same gas-phase modification method but opting for a monofunctional amine instead of a bifunctional amine, some authors have succeeded in increasing the adsorption capacity of nanocellulose aerogel by 1 mol (Jia et al., 2022).

The configuration of the introduced amine on the surface of the aerogel can notably improve the CO_2 adsorption rate. The use of a nonlinear amine, containing an aromatic group such as phthalamide, has achieved the best-reported rates so far (Sepahvand et al., 2020). This modify nanaocellulose aerogel incorporates a range of chemical functionalities, including carbonyl groups and aromatic amines offering high

affinity with the CO_2 molecules. However, comparing existing studies is challenging as they often omit quantifying the molar rate of introduced amine on nanocellulose aerogels. Additionally, the method for quantifying the adsorption rate is not yet standardized by the IUPAC, hindering a proper comparison of achieved adsorption rates.

Regarding the development of hybrid nanocellulose aerogels, studies conducted so far show lower adsorption rates compared to purely modified nanocellulose aerogels, not providing a significant impact. However, as reported above, some authors have explored the development of hybrid aerogels by combining graphene oxide, poly(vinyl alcohol) and nanocellulose. This research has led to the creation of high-performance aerogels, using a carbonization step to generate a high-surface-area, micropore-rich structure (Zhang et al., 2022). Thanks to this micropores, this aerogel achieved a remarkable CO_2 adsorption of 19.32 mmol/g. However, this exceptional performance raises important questions about the sustainability and environmental viability of the method, particularly due to the use of an energy-intensive carbonization step. This perspective raises a key question: is it wise to focus on potentially high-performance hybrid materials despite energy-intensive processes, or should we not instead focus our efforts on developing entirely green materials, combined with environmentally-friendly processes? The balance between performance and sustainability needs to be carefully assessed to determine the most responsible path in the development of nanocellulose aerogels, taking into account current ecological requirements.

7. Conclusions and future challenges

The urgent requirement to tackle climate change and mitigate greenhouse gas emissions has driven the creation of inventive materials that combine sustainable production with efficient CO_2 capture. To this end, the use of porous materials for adsorption is a promising strategy to capture CO_2. In this regard, aerogels have been widely investigated and examined for their adsorption capacity. Aerogels are very well-engineered porous materials with high surface area, controllable pore size, and high adsorption capacity. In this review, we explore the growing trend of using nanocellulose aerogels for carbon dioxide adsorption. The use of cellulose as raw material for aerogel production is a key element in reducing the carbon footprint and shifting toward green chemistry strategy by limiting the use of non-renewable feedstocks. CO_2 adsorption by nanocellulose aerogels occurs via physisorption through low energy Van der Waals interactions between the adsorbent and the CO_2 molecules. Chemical modification of nanocellulose with amine moieties enhances the adsorption capacity by providing a large number of active binding sites that promote interactions between the aerogel and the CO_2 molecules. A zwitterion mechanism is commonly reported to describe the interaction between CO_2 and primary/secondary amines. However, industrial scale production and achieving high adsorption capacity still present some challenges:

- The current methods of extracting nanocellulose is a multi-step process that involves the use of expensive and toxic chemicals, making its large-scale production harmful and expensive. Consequently, less toxic methods for the production of nanocellulose should be explored. Recent advances in green pre-treatment methods for the production of nanocellulose have shown promise in reducing the cost of the extraction process. Therefore, the prospects for large-scale production of nanocellulose are encouraging.
- Functionalization of nanocelullose aerogels with amines turns out to be an efficient strategy to improve the adsorption rates of CO_2 molecules. However, the grafted amines remain relatively unstable which impede high adsorption efficiency. A comprehensive screening of amines groups employed for the synthesis of nanocellulose adsorbents should be therefore conducted to elucidate the link between high adsorption capacity and stability upon regeneration.

- Despite the enormous amount of research that exists on the synthesis of nanonocellulose aerogels, the commercialization of aerogels remains a challenge. Supercritical drying which stands as the method of choice for manufacturing nanocellulose-based aerogels is inherently energy intensive. Consequently, resulting materials are generally not economically viable. Thus, the overall process for nanocellulose-based aerogel should be optimized to match with the requirement of commercial development.
- Specific analytical and simulation tools must be developed to screen and approve aerogel synthesis, estimate material properties, and better understand the CO_2/aerogels interactions.
- Another major challenge is to enhance the mechanical stability of aerogels up to industry requirements. It is mandatory to explore methods to make aerogels structurally robust. One possible solution would be to develop lignocellulose-based aerogels containing amorphous lignin fractions that can increase the strength and the long-term structural stability of aerogels.

Abbreviations

CO_2	carbon dioxide
CO	Carbone monoxide
sc-CO_2	supercritical carbon dioxide
SF	silk fibroin
CNFs	cellulose nanofibers
CNCs	cellulose nanocrystals
BNC	bacterial nanocellulose
IT	ice templating
3D	three dimensional
BET	Brunauer–Emmett–Teller
BJH	Barrett-Joyner-Halenda
DFT	Density Functional Theory
SEM	scanning electron microscopy
AEAPMDS	N-(2-aminoethyl)-3-aminopropyl-methyl dimethoxysilane
APMDS	3-aminopropyl-methyl diethoxysilane
S_{BET}	BET's specific surface area
TEMPO	(2,2,6,6-tetramethylpiperidin-1-yl)oxy
APTES	(3-Aminopropyl)triethoxysilane
MOFs	metal-organic frameworks
ZIF-L	zeolitic imidazolate
GO	graphene oxide
konjac	glucomannan/nanofiber
PVA	polyvinyl acetate
CCS	carbon dioxide capture and storage

CRediT authorship contribution statement

Farida Baraka: Data curation, Investigation, Writing – original draft. **Jalel Labidi:** Investigation, Supervision, Writing – review & editing.

Declaration of competing interest

The authors declare that they have no known competing financial interests or personal relationships that could have appeared to influence the work reported in this paper.

Data availability

No data was used for the research described in the article.

Acknowledgments

References

Ahmed, M.S., Attia, Y.A., 1998. Multi-metal oxide aerogel for capture of pollution gases from air. Appl. Therm. Eng. 18, 787–797. https://doi.org/10.1016/S1359-4311(97)00104-X.

Aljamali, N., Khdur, R., Alfatlawi, I., 2021. Physical and Chemical Adsorption and Its Applications, 7, pp. 1–8. https://doi.org/10.37628/IJTCK.

Anas, M., Gönel, A.G., Bozbag, S.E., Erkey, C., 2017. Thermodynamics of adsorption of carbon dioxide on various aerogels. J. CO2 Util. 21, 82–88. https://doi.org/10.1016/j.jcou.2017.06.008.

Ayral, A., Phalippou, J., Woignier, T., 1992. Skeletal density of silica aerogels determined by helium pycnometry. J. Mater. Sci. 27, 1166–1170. https://doi.org/10.1007/BF01142014.

Belmabkhout, Y., Guillerm, V., Eddaoudi, M., 2016. Low concentration CO2 capture using physical adsorbents: are metal–organic frameworks becoming the new benchmark materials? Chem. Eng. J. 296, 386–397. https://doi.org/10.1016/j.cej.2016.03.124.

Benselfelt, T., Wågberg, L., 2019. Unidirectional swelling of dynamic cellulose nanofibril networks: a platform for tunable hydrogels and aerogels with 3D shapeability. Biomacromolecules 20, 2406–2412. https://doi.org/10.1021/acs.biomac.9b00401.

Bhatti, U.H., Sivanesan, D., Lim, D.H., Nam, S.C., Park, S., Baek, I.H., 2018. Metal oxide catalyst-aided solvent regeneration: a promising method to economize post-combustion CO2 capture process. J. Taiwan Inst. Chem. Eng. 93, 150–157. https://doi.org/10.1016/j.jtice.2018.05.029.

Brunauer, S., Emmett, P.H., Teller, E., 1938. Adsorption of gases in multimolecular layers. J. Am. Chem. Soc. 60, 309–319. https://doi.org/10.1021/ja01269a023.

Buchtová, N., Budtova, T., 2016. Cellulose aero-, cryo- and xerogels: towards understanding of morphology control. Cellulose 23, 2585–2595. https://doi.org/10.1007/s10570-016-0960-8.

Bui, M., Adjiman, C.S., Bardow, A., Anthony, E.J., Boston, A., Brown, S., Fennell, P.S., Fuss, S., Galindo, A., Hackett, L.A., Hallett, J.P., Herzog, H.J., Jackson, G., Kemper, J., Krevor, S., Maitland, G.C., Matuszewski, M., Metcalfe, I.S., Petit, C., Puxty, G., Reimer, J., Reiner, D.M., Rubin, E.S., Scott, S.A., Shah, N., Smit, B., Trusler, J.P.M., Webley, P., Wilcox, J., Mac Dowell, N., 2018. Carbon capture and storage (CCS): the way forward. Energ. Environ. Sci. 11, 1062–1176. https://doi.org/10.1039/C7EE02342A.

Campbell, L.K., Na, B.K., Ko, E.I., 1992. Synthesis and characterization of titania aerogels. Chem. Mater. 4, 1329–1333. https://doi.org/10.1021/cm00024a037.

Chen, H., 2014. Chemical Composition and Structure of Natural Lignocellulose, pp. 25–71. https://doi.org/10.1007/978-94-007-6898-7_2.

Chen, C., Zhang, S., Row, K.H., Ahn, W.-S., 2017. Amine–silica composites for CO2 capture: a short review. J. Energy Chem. 26, 868–880. https://doi.org/10.1016/j.jechem.2017.07.001.

Chen, L., Gong, M., Cheng, Y., Liu, Y., Yin, S., Luo, D., 2019. Effect of pore structure of supports on CO2 adsorption of tetraethylenepentamine/carbon aerogels prepared by incipient wetness impregnation method. Polish J. Environ. Stud. 28, 4127–4137. https://doi.org/10.15244/pjoes/98997.

Chen, Y., Zhang, L., Yang, Y., Pang, B., Xu, W., Duan, G., Jiang, S., Zhang, K., 2021. Recent progress on nanocellulose aerogels: preparation, modification, composite fabrication, applications. Adv. Mater. 33, 2005569 https://doi.org/10.1002/adma.202005569.

Cheng, Z., DeGracia, K., Schiraldi, D., 2018. Sustainable, low flammability, mechanically-strong poly(vinyl alcohol) aerogels. Polymers (Basel) 10, 1102. https://doi.org/10.3390/polym10101102.

CO₂ Emissions | Energy Economics | Home [WWW Document]. n.d. URL. https://www.bp.com/en/global/corporate/energy-economics/statistical-review-of-world-energy/co2-emissions.html (accessed 2.20.23).

Coquard, R., Baillis, D., Quenard, D., 2006. Experimental and theoretical study of the hot-wire method applied to low-density thermal insulators. Int. J. Heat Mass Transf. 49, 4511–4524. https://doi.org/10.1016/j.ijheatmasstransfer.2006.05.016.

Dassanayake, R.S., Gunathilake, C., Abidi, N., Jaroniec, M., 2018. Activated carbon derived from chitin aerogels: preparation and CO2 adsorption. Cellulose 25, 1911–1920. https://doi.org/10.1007/s10570-018-1660-3.

De France, K.J., Hoare, T., Cranston, E.D., 2017. Review of hydrogels and aerogels containing nanocellulose. Chem. Mater. 29, 4609–4631. https://doi.org/10.1021/acs.chemmater.7b00531.

Deshpande, R., Hua, D.-W., Smith, D.M., Brinker, C.J., 1992. Pore structure evolution in silica gel during aging/drying. III. Effects of surface tension. J. Non Cryst. Solids 144, 32–44. https://doi.org/10.1016/S0022-3093(05)80380-1.

Deville, S., 2010. Freeze-casting of porous biomaterials: structure, properties and opportunities. Materials (Basel). https://doi.org/10.3390/ma3031913.

Economics, Statistical Review of World Energy [WWW Document]. n.d. URL. https://www.bp.com/en/global/corporate/energy-economics/statistical-review-of-world-energy/co2-emissions.html. (Accessed 2 October 2023).

Fall, A.B., Lindström, S.B., Sundman, O., Ödberg, L., Wågberg, L., 2011. Colloidal stability of aqueous nanofibrillated cellulose dispersions. Langmuir 27, 11332–11338. https://doi.org/10.1021/la201947x.

Ganesan, K., Dennstedt, A., Barowski, A., Ratke, L., 2016. Design of aerogels, cryogels and xerogels of cellulose with hierarchical porous structures. Mater. Des. 92, 345–355. https://doi.org/10.1016/j.matdes.2015.12.041.

Gebald, C., Wurzbacher, J.A., Tingaut, P., Zimmermann, T., Steinfeld, A., 2011. Amine-based nanofibrillated cellulose as adsorbent for CO2 capture from air. Environ. Sci. Technol. 45, 9101–9108. https://doi.org/10.1021/es202223p.

Gebald, C., Wurzbacher, J.A., Borgschulte, A., Zimmermann, T., Steinfeld, A., 2014. Single-component and binary CO2 and H2O adsorption of amine-functionalized

cellulose. Environ. Sci. Technol. 48, 2497–2504. https://doi.org/10.1021/es404430g.

Geng, S., Maennlein, A., Yu, L., Hedlund, J., Oksman, K., 2021. Monolithic carbon aerogels from bioresources and their application for CO2 adsorption. Microporous Mesoporous Mater. 323, 111236 https://doi.org/10.1016/j.micromeso.2021.111236.

Guarín Romero, J.R., Moreno-Piraján, J.C., Giraldo Gutierrez, L., 2018. Kinetic and equilibrium study of the adsorption of CO2 in ultramicropores of resorcinol-formaldehyde aerogels obtained in acidic and basic medium. C. https://doi.org/10.3390/c4040052.

Hart, A., Gnanendran, N., 2009. Cryogenic CO2 capture in natural gas. Energy Procedia 1, 697–706. https://doi.org/10.1016/j.egypro.2009.01.092.

Ho, N.A.D., Leo, C.P., 2021. A review on the emerging applications of cellulose, cellulose derivatives and nanocellulose in carbon capture. Environ. Res. 197, 111100 https://doi.org/10.1016/j.envres.2021.111100.

Horvat, G., Pantić, M., Knez, Ž., Novak, Z., 2022. A brief evaluation of pore structure determination for bioaerogels. Gels. https://doi.org/10.3390/gels8070438.

Huang, H.-P., Wright, I.P., Gilmour, I., Pillinger, C.T., 1994. Supercritical fluid extraction as a means of reducing the carbon contamination inherent in samples of silica aerogel destined for the capture of CHON cosmic dust particles in space. Planet. Space Sci. 42, 947–954. https://doi.org/10.1016/0032-0633(94)90055-8.

Husain, F.M., Khan, Altaf, Khan, R.A., Siddique, J.A., Oves, M., Khan, A.A.P., Ansari, M. O., Cancar, H.D., 2021. In: Khan, A.A.P., Ansari, M.O., Khan, Anish, Asiri, A.M.B.T.-A. in A.C. for E.R. (Eds.), Chapter 18 - Bio-based Aerogels and Their Environment Applications: An Overview. Elsevier, pp. 347–356. https://doi.org/10.1016/B978-0-12-820732-1.00018-7.

Illera, D., Mesa, J., Gomez, H., Maury, H., 2018. Cellulose aerogels for thermal insulation in buildings: trends and challenges. Coatings. https://doi.org/10.3390/coatings8100345.

Jia, P., Xu, J., Wang, X., Chen, Z., Xie, Z., Jiang, H., 2022. Comparison of characteristics of the cellulose nanocrystal aerogels aminosilane-functionalized through gas-phase reaction. J. Porous. Mater. 29, 745–758. https://doi.org/10.1007/s10934-022-01209-1.

Jiang, F., Hu, S., Hsieh, Y., 2018. Aqueous synthesis of compressible and thermally stable cellulose nanofibril–silica aerogel for CO2 adsorption. ACS Appl. Nano Mater. 1, 6701–6710. https://doi.org/10.1021/acsanm.8b01515.

Jiménez-Saelices, C., Seantier, B., Cathala, B., Grohens, Y., 2017. Spray freeze-dried nanofibrillated cellulose aerogels with thermal superinsulating properties. Carbohydr. Polym. 157, 105–113. https://doi.org/10.1016/j.carbpol.2016.09.068.

Joyner, L.G., Barrett, E.P., Skold, R., 1951. The determination of pore volume and area distributions in porous substances. II. Comparison between nitrogen isotherm and mercury porosimeter methods. J. Am. Chem. Soc. 73, 3155–3158. https://doi.org/10.1021/ja01151a046.

Kanniche, M., Gros-Bonnivard, R., Jaud, P., Valle-Marcos, J., Amann, J.-M., Bouallou, C., 2010. Pre-combustion, post-combustion and oxy-combustion in thermal power plant for CO2 capture. Appl. Therm. Eng. 30, 53–62. https://doi.org/10.1016/j.applthermaleng.2009.05.005.

Kecili, R., Hussain, C.M., 2018. In: Hussain, C.M.B.T.-N. in C. (Ed.), Chapter 4 - Mechanism of Adsorption on Nanomaterials. Elsevier, pp. 89–115. https://doi.org/10.1016/B978-0-12-812792-6.00004-2.

Keller, J.U., Staudt, R. (Eds.), 2005. Adsorption Isotherms BT - Gas Adsorption Equilibria: Experimental Methods and Adsorptive Isotherms. Springer US, Boston, MA, pp. 359–413. https://doi.org/10.1007/0-387-23598-1_8.

Keshavarz, L., Ghaani, M.R., MacElroy, J.M.D., English, N.J., 2021. A comprehensive review on the application of aerogels in CO2-adsorption: materials and characterisation. Chem. Eng. J. 412, 128604 https://doi.org/10.1016/j.cej.2021.128604.

Kistler, S.S., 1931. Coherent expanded aerogels and jellies. Nature 127, 741. https://doi.org/10.1038/127741a0.

Kong, Y., Jiang, G., Fan, M., Shen, X., Cui, S., 2014. Use of one-pot wet gel or precursor preparation and supercritical drying procedure for development of a high-performance CO2 sorbent. RSC Adv. 4, 43448–43453. https://doi.org/10.1039/C4RA07120D.

Kong, Y., Shen, X., Fan, M., Yang, M., Cui, S., 2016. Dynamic capture of low-concentration CO2 on amine hybrid silsesquioxane aerogel. Chem. Eng. J. 283, 1059–1068. https://doi.org/10.1016/j.cej.2015.08.034.

Lastoskie, C., Gubbins, K.E., Quirke, N., 1993. Pore size distribution analysis of microporous carbons: a density functional theory approach. J. Phys. Chem. 97, 4786–4796. https://doi.org/10.1021/j100120a035.

Lavoine, N., Bergström, L., 2017. Nanocellulose-based foams and aerogels: processing, properties, and applications. J. Mater. Chem. A 5, 16105–16117. https://doi.org/10.1039/C7TA02807E.

Lee, J.-H., Park, S.-J., 2020. Recent advances in preparations and applications of carbon aerogels: a review. Carbon N. Y. 163, 1–18. https://doi.org/10.1016/j.carbon.2020.02.073.

Li, Y., Jia, P., Xu, J., Wu, Y., Jiang, H., Li, Z., 2020. The aminosilane functionalization of cellulose nanofibrils and the mechanical and CO2 adsorption characteristics of their aerogel. Ind. Eng. Chem. Res. 59, 2874–2882. https://doi.org/10.1021/acs.iecr.9b04253.

Liebner, F., Potthast, A., Rosenau, T., Haimer, E., Wendland, M., 2007. Ultralight-weight cellulose aerogels from NBnMO-stabilized lyocell dopes. Res. Lett. Mater. Sci. 2007, 73724. https://doi.org/10.1155/2007/73724.

Lin, J., Li, G., Liu, W., Qiu, R., Wei, H., Zong, K., Cai, X., 2021. A review of recent progress on the silica aerogel monoliths: synthesis, reinforcement, and applications. J. Mater. Sci. 56, 10812–10833. https://doi.org/10.1007/s10853-021-05997-w.

Linneen, N., 2014. Synthesis and Carbon Dioxide Adsorption Properties of Amine Modified Particulate Silica Aerogel Sorbents. Arizona State University.

Linneen, N.N., Pfeffer, R., Lin, Y.S., 2014. CO2 adsorption performance for amine grafted particulate silica aerogels. Chem. Eng. J. 254, 190–197. https://doi.org/10.1016/j.cej.2014.05.087.

Liu, A., Medina, L., Berglund, L.A., 2017. High-strength nanocomposite aerogels of ternary composition: poly(vinyl alcohol), clay, and cellulose nanofibrils. ACS Appl. Mater. Interfaces 9, 6453–6461. https://doi.org/10.1021/acsami.6b15561.

Liu, S., Zhang, Y., Jiang, H., Wang, X., Zhang, T., Yao, Y., 2018. High CO2 adsorption by amino-modified bio-spherical cellulose nanofibres aerogels. Environ. Chem. Lett. 16, 605–614. https://doi.org/10.1007/s10311-017-0701-8.

Liu, Z., Ran, Y., Xi, J., Wang, J., 2020. Polymeric hybrid aerogels and their biomedical applications. Soft Matter 16, 9160–9175. https://doi.org/10.1039/D0SM01261K.

Liu, Z., Zhang, S., He, B., Wang, S., Kong, F., 2021. Synthesis of cellulose aerogels as promising carriers for drug delivery: a review. Cellulose 28, 2697–2714. https://doi.org/10.1007/s10570-021-03734-9.

Long, L., Weng, Y.-X., Wang, Y.-Z., 2018. Cellulose aerogels: synthesis, applications, and prospects. Polymers (Basel) 10, 623. https://doi.org/10.3390/polym10060623.

Mankar, A.R., Pandey, A., Modak, A., Pant, K.K., 2021. Pretreatment of lignocellulosic biomass: a review on recent advances. Bioresour. Technol. 334, 125235 https://doi.org/10.1016/j.biortech.2021.125235.

Marques, L.M., Carrott, P.J.M., Carrott, M.M.L.R., 2016. Carbon aerogels used in carbon dioxide capture. Boletín del Grup. Español del Carbón 9–12.

Martín, C.F., Sweatman, M.B., Brandani, S., Fan, X., 2016. Wet impregnation of a commercial low cost silica using DETA for a fast post-combustion CO2 capture process. Appl. Energy 183, 1705–1721. https://doi.org/10.1016/j.apenergy.2016.09.081.

Martoia, F., Cochereau, T., Dumont, P., Orgéas, L., Terrien, M., Belgacem, N., 2016. Cellulose nanofibrils foams: links between ice-templating conditions, microstructures and mechanical properties. Mater. Des. 104, 376–391. https://doi.org/10.1016/j.matdes.2016.04.088.

Meador, M.A.B., Wright, S., Sandberg, A., Nguyen, B.N., Van Keuls, F.W., Mueller, C.H., Rodríguez-Solís, R., Miranda, F.A., 2012. Low dielectric polyimide aerogels as substrates for lightweight patch antennas. ACS Appl. Mater. Interfaces 4, 6346–6353. https://doi.org/10.1021/am301985s.

Moon, R.J., Martini, A., Nairn, J., Simonsen, J., Youngblood, J., 2011. Cellulose nanomaterials review: structure, properties and nanocomposites. Chem. Soc. Rev. 40, 3941–3994. https://doi.org/10.1039/C0CS00108B.

Munier, P., Gordeyeva, K., Bergström, L., Fall, A.B., 2016. Directional freezing of nanocellulose dispersions aligns the rod-like particles and produces low-density and robust particle networks. Biomacromolecules 17, 1875–1881. https://doi.org/10.1021/acs.biomac.6b00304.

Nagarajan, K., Ramanujam, N., M R, S., Siengchin, S., Balachandran, S., Kathar, S., Madhu, P., G R, R., 2020. A comprehensive review on cellulose nanocrystals and cellulose nanofibers: pretreatment, preparation and characterization. Polym. Compos. 42, 1588–1630. https://doi.org/10.1002/pc.25929.

Nakao, S., Yogo, K., Goto, K., Kai, T., Yamada, H., 2019. In: Nakao, S., Yogo, K., Goto, K., Kai, T., Yamada, H. (Eds.), CO2 Capture with Absorbents BT - Advanced CO2 Capture Technologies: Absorption, Adsorption, and Membrane Separation Methods. Springer International Publishing, Cham, pp. 23–44. https://doi.org/10.1007/978-3-030-18858-0_3.

Ogungbenro, A.E., Quang, D.V., Al-Ali, K., Abu-Zahra, M.R.M., 2017. Activated carbon from date seeds for CO2 capture applications. Energy Procedia 114, 2313–2321. https://doi.org/10.1016/j.egypro.2017.03.1370.

Pääkkö, M., Vapaavuori, J., Silvennoinen, R., Kosonen, H., Ankerfors, M., Lindström, T., Berglund, L.A., Ikkala, O., 2008. Long and entangled native cellulose I nanofibers allow flexible aerogels and hierarchically porous templates for functionalities. Soft Matter 4, 2492–2499. https://doi.org/10.1039/B810371B.

Pajonk, G.M., Venkateswara Rao, A., Parvathy, N.N., Elaloui, E., 1996. Microstructural characterization of silica aerogels using scanning electron microscopy. J. Mater. Sci. 31, 5683–5689. https://doi.org/10.1007/BF01160815.

Pierre, A.C., Pajonk, G.M., 2002. Chemistry of aerogels and their applications. Chem. Rev. 102, 4243–4266. https://doi.org/10.1021/cr0101306.

Pour, G., Beauger, C., Rigacci, A., Budtova, T., 2015. Xerocellulose: lightweight, porous and hydrophobic cellulose prepared via ambient drying. J. Mater. Sci. 50, 4526–4535. https://doi.org/10.1007/s10853-015-9002-4.

Powell, C.E., Qiao, G.G., 2006. Polymeric CO2/N2 gas separation membranes for the capture of carbon dioxide from power plant flue gases. J. Memb. Sci. 279, 1–49. https://doi.org/10.1016/j.memsci.2005.12.062.

Querejeta, N., Gil, M.V., Pevida, C., Centeno, T.A., 2018. Standing out the key role of ultramicroporosity to tailor biomass-derived carbons for CO2 capture. J. CO2 Util. 26, 1–7. https://doi.org/10.1016/j.jcou.2018.04.016.

Reichenauer, G., 2011. In: Aegerter, M.A., Leventis, N., Koebel, M.M. (Eds.), Structural Characterization of Aerogels BT - Aerogels Handbook. Springer New York, New York, NY, pp. 449–498. https://doi.org/10.1007/978-1-4419-7589-8_21.

Rigacci, A., Achard, P., 2011. Cellulosic and Polyurethane Aerogels, pp. 191–214. https://doi.org/10.1007/978-1-4419-7589-8_10.

Rollins, H., Bunker, C., Yaping, S., Meziani, J., Bandara, J., 2002. Preparation and Processing of Nanoscale Materials by Supercritical Fluid Technology. https://doi.org/10.1201/9780203909362.ch13.

Rostami, J., Benselfelt, T., Maddalena, L., Avci, C., Sellman, F.A., Cinar Ciftci, G., Larsson, C., Carosio, F., Akhtar, F., Tian, W., Wågberg, L., 2022. Shaping 90 wt% nanoMOFs into robust multifunctional aerogels using tailored bio-based nanofibrils. Adv. Mater. 34, 2204800 https://doi.org/10.1002/adma.202204800.

Rottmann, M., Beikircher, T., Ebert, H.-P., 2020. Thermal conductivity of evacuated expanded perlite measured with guarded-hot-plate and transient-hot-wire method at

temperatures between 295 K and 1073 K. Int. J. Therm. Sci. 152, 106338 https://doi.org/10.1016/j.ijthermalsci.2020.106338.

Sai Bhargava Reddy, M., Ponnamma, D., Sadasivuni, K.K., Kumar, B., Abdullah, A.M., 2021. Carbon dioxide adsorption based on porous materials. RSC Adv. 11, 12658–12681. https://doi.org/10.1039/D0RA10902A.

Said, R. Ben, Kolle, J.M., Essalah, K., Tangour, B., Sayari, A., 2020. A unified approach to CO2–amine reaction mechanisms. ACS Omega 5, 26125–26133. https://doi.org/10.1021/acsomega.0c03727.

Scherer, G.W., 1986. Drying gels: I. General theory. J. Non. Cryst. Solids 87, 199–225. https://doi.org/10.1016/S0022-3093(86)80079-5.

Scherer, G.W., 1998. Adsorption in aerogel networks. J. Non Cryst. Solids 225, 192–199. https://doi.org/10.1016/S0022-3093(98)00117-3.

Sehaqui, H., Zhou, Q., Berglund, L.A., 2011. High-porosity aerogels of high specific surface area prepared from nanofibrillated cellulose (NFC). Compos. Sci. Technol. 71, 1593–1599. https://doi.org/10.1016/j.compscitech.2011.07.003.

Sepahvand, S., Jonoobi, M., Ashori, A., Gauvin, F., Brouwers, H.J.H., Oksman, K., Yu, Q., 2020. A promising process to modify cellulose nanofibers for carbon dioxide (CO2) adsorption. Carbohydr. Polym. 230, 115571 https://doi.org/10.1016/j.carbpol.2019.115571.

Sepahvand, S., Kargarzadeh, H., Jonoobi, M., Ashori, A., Ismaeilimoghadam, S., Varghese, R.T., Chirayl, C.J., Azimi, B., Danti, S., 2023. Recent developments in nanocellulose-based aerogels as air filters: a review. Int. J. Biol. Macromol. 246, 125721 https://doi.org/10.1016/j.ijbiomac.2023.125721.

Shen, J., Wang, J., Zhai, J., Guo, Y., Wu, G., Zhou, B., Ni, X., 2004. Carbon aerogel films synthesized at ambient conditions. J. Sol-Gel Sci. Technol. 31, 209–213. https://doi.org/10.1023/B:JSST.0000047989.39431.d5.

Song, Z., Zhao, H., 2018. Preparation and characterization of mullite-silica aerogel composite material. Open J. Org. Polym. Mater. 08, 43–52. https://doi.org/10.4236/ojopm.2018.84004.

Song, J., Liu, J., Zhao, W., Chen, Y., Xiao, H., Shi, X., Liu, Y., Chen, X., 2018. Quaternized chitosan/PVA aerogels for reversible CO2 capture from ambient air. Ind. Eng. Chem. Res. 57, 4941–4948. https://doi.org/10.1021/acs.iecr.8b00064.

Sun, J., Shang, M., Zhang, M., Yu, S., Yuan, Z., Yi, X., Filatov, S., Zhang, J., 2022. Konjac glucomannan/cellulose nanofibers composite aerogel supported HKUST-1 for CO2 adsorption. Carbohydr. Polym. 293, 119720 https://doi.org/10.1016/j.carbpol.2022.119720.

Svensson, A., Larsson, P.T., Salazar-Alvarez, G., Wågberg, L., 2013. Preparation of dry ultra-porous cellulosic fibres: characterization and possible initial uses. Carbohydr. Polym. 92, 775–783. https://doi.org/10.1016/j.carbpol.2012.09.090.

Teichner, S.J., Nicolaon, G.A., Vicarini, M.A., Gardes, G.E.E., 1976. Inorganic oxide aerogels. Adv. Colloid Interface Sci. 5, 245–273. https://doi.org/10.1016/0001-8686(76)80004-8.

Ummartyotin, S., Manuspiya, H., 2015. A critical review on cellulose: from fundamental to an approach on sensor technology. Renew. Sustain. Energy Rev. 41, 402–412. https://doi.org/10.1016/j.rser.2014.08.050.

Valencia, L., Abdelhamid, H.N., 2019. Nanocellulose leaf-like zeolitic imidazolate framework (ZIF-L) foams for selective capture of carbon dioxide. Carbohydr. Polym. 213, 338–345. https://doi.org/10.1016/j.carbpol.2019.03.011.

Valencia, L., Rosas, W., Aguilar-Sanchez, A., Mathew, A.P., Palmqvist, A.E.C., 2019. Bio-based micro-/meso-/macroporous hybrid foams with ultrahigh zeolite loadings for selective capture of carbon dioxide. ACS Appl. Mater. Interfaces 11, 40424–40431. https://doi.org/10.1021/acsami.9b11399.

van de Witte, P., Dijkstra, P.J., van den Berg, J.W.A., Feijen, J., 1996. Phase separation processes in polymer solutions in relation to membrane formation. J. Membr. Sci. 117, 1–31. https://doi.org/10.1016/0376-7388(96)00088-9.

Verma, A., Thakur, S., Goel, G., Raj, J., Gupta, V.K., Roberts, D., Thakur, V.K., 2020. Bio-based sustainable aerogels: new sensation in CO2 capture. Curr. Res. Green Sustain. Chem. 3, 100027 https://doi.org/10.1016/j.crgsc.2020.100027.

Walker, R.C., Potochniak, A.E., Hyer, A.P., Ferri, J.K., 2021. Zirconia aerogels for thermal management: review of synthesis, processing, and properties information architecture. Adv. Colloid Interface Sci. 295, 102464 https://doi.org/10.1016/j.cis.2021.102464.

Wang, M., Lawal, A., Stephenson, P., Sidders, J., Ramshaw, C., 2011. Post-combustion CO2 capture with chemical absorption: a state-of-the-art review. Chem. Eng. Res. Des. 89, 1609–1624. https://doi.org/10.1016/j.cherd.2010.11.005.

Wang, Q., Feng, J., Ma, L., Xie, J., Xia, C., Zhu, J., Jiang, D., 2016. Synthesis, characterization, and adsorption properties of silica aerogels crosslinked with diisocyanate under ambient drying. J. Mater. Sci. 51 https://doi.org/10.1007/s10853-016-0191-2.

Wang, Y., Su, Y., Wang, W., Fang, Y., Riffat, S.B., Jiang, F., 2019. The advances of polysaccharide-based aerogels: preparation and potential application. Carbohydr. Polym. 226, 115242 https://doi.org/10.1016/j.carbpol.2019.115242.

Wang, Z., Zhu, W., Huang, R., Zhang, Y., Jia, C., Zhao, H., Chen, W., Xue, Y., 2020. Fabrication and characterization of cellulose nanofiber aerogels prepared via two different drying techniques. Polymers (Basel). https://doi.org/10.3390/polym12112583.

Wei, J., Geng, S., Hedlund, J., Oksman, K., 2020. Lightweight, flexible, and multifunctional anisotropic nanocellulose-based aerogels for CO2 adsorption. Cellulose 27, 2695–2707. https://doi.org/10.1007/s10570-019-02935-7.

Wei, G., Zhang, J., Usuelli, M., Zhang, X., Liu, B., Mezzenga, R., 2022. Biomass vs inorganic and plastic-based aerogels: structural design, functional tailoring, resource-efficient applications and sustainability analysis. Prog. Mater. Sci. 125, 100915 https://doi.org/10.1016/j.pmatsci.2021.100915.

Wörmeyer, K., Alnaief, M., Smirnova, I., 2012. Amino functionalised silica-aerogels for CO2-adsorption at low partial pressure. Adsorption 18, 163–171. https://doi.org/10.1007/s10450-012-9390-6.

Wu, X.-L., Xu, A.-W., 2014. Carbonaceous hydrogels and aerogels for supercapacitors. J. Mater. Chem. A 2, 4852–4864. https://doi.org/10.1039/C3TA13929H.

Wu, Y., Cao, F., Jiang, H., Zhang, Y., 2017. Preparation and characterization of aminosilane-functionalized cellulose nanocrystal aerogel. Mater. Res. Express 4, 85303. https://doi.org/10.1088/2053-1591/aa8067.

Wu, Y., Zhang, Y., Chen, N., Dai, S., Jiang, H., Wang, S., 2018. Effects of amine loading on the properties of cellulose nanofibrils aerogel and its CO2 capturing performance. Carbohydr. Polym. 194, 252–259. https://doi.org/10.1016/j.carbpol.2018.04.017.

Xiao, S., Gao, R., Lu, Y., Li, J., Sun, Q., 2015. Fabrication and characterization of nanofibrillated cellulose and its aerogels from natural pine needles. Carbohydr. Polym. 119, 202–209. https://doi.org/10.1016/j.carbpol.2014.11.041.

Xu, J., Jia, P., Wang, X., Xie, Z., Chen, Z., Jiang, H., 2021. The aminosilane functionalization of cellulose nanocrystal aerogel via vapor-phase reaction and its CO2 adsorption characteristics. J. Appl. Polym. Sci. 138, 50891. https://doi.org/10.1002/app.50891.

Xu, Yang, Xu, Yongjian, Chen, H., Gao, M., Yue, X., Ni, Y., 2022. Redispersion of dried plant nanocellulose: a review. Carbohydr. Polym. 294, 119830 https://doi.org/10.1016/j.carbpol.2022.119830.

Yamashita, J., Ojima, T., Shioya, M., Hatori, H., Yamada, Y., 2003. Organic and carbon aerogels derived from poly(vinyl chloride). Carbon N. Y. 41, 285–294. https://doi.org/10.1016/S0008-6223(02)00289-0.

Yaqub, S., Pei, L.S., Mellon, N., Shariff, A.M., 2016. Performance evaluation of covalent organic polymer adsorbent prepared via microwave technique for CO2 and CH4 adsorption. Proc. Eng. 148, 249–253. https://doi.org/10.1016/j.proeng.2016.06.604.

Yu, J., Zhai, Y., Chuang, S.S.C., 2018. Water enhancement in CO2 capture by amines: an insight into CO2–H2O interactions on amine films and sorbents. Ind. Eng. Chem. Res. 57, 4052–4062. https://doi.org/10.1021/acs.iecr.7b05114.

Yurduşen, A., Yürüm, A., Yürüm, Y., 2020. The role of ultramicropores in the CO2 adsorption capacity of Fe–BTC crystallites synthesized with a perturbation-assisted nanofusion synthesis strategy. CrystEngComm 22, 932–944. https://doi.org/10.1039/C9CE01626K.

Zhang, H., Goeppert, A., Olah, G.A., Prakash, G.K.S., 2017. Remarkable effect of moisture on the CO2 adsorption of nano-silica supported linear and branched polyethylenimine. J. CO2 Util. 19, 91–99. https://doi.org/10.1016/j.jcou.2017.03.008.

Zhang, T., Zhang, Y., Jiang, H., Wang, X., 2019. Aminosilane-grafted spherical cellulose nanocrystal aerogel with high CO2 adsorption capacity. Environ. Sci. Pollut. Res. 26, 16716–16726. https://doi.org/10.1007/s11356-019-05068-3.

Zhang, T., Zhang, W., Zhang, Y., Shen, M., Zhang, J., 2020. Gas phase synthesis of aminated nanocellulose aerogel for carbon dioxide adsorption. Cellulose 27, 2953–2958. https://doi.org/10.1007/s10570-020-03035-7.

Zhang, Q., Lu, W., Wu, M., Qi, G., Yuan, Y., Li, J., Su, H., Zhang, H., 2022. Preparation and properties of cellulosenanofiber (CNF)/polyvinyl alcohol (PVA)/graphene oxide (GO): application of CO2 absorption capacity and molecular dynamics simulation. J. Environ. Manage. 302, 114044 https://doi.org/10.1016/j.jenvman.2021.114044.

Zhou, T., Cheng, X., Pan, Y., Li, C., Gong, L., 2019. Mechanical performance and thermal stability of polyvinyl alcohol–cellulose aerogels by freeze drying. Cellulose 26. https://doi.org/10.1007/s10570-018-2179-3.

Zhu, W., Yao, Y., Zhang, Y., Jiang, H., Wang, Z., Chen, W., Xue, Y., 2020. Preparation of an amine-modified cellulose nanocrystal aerogel by chemical vapor deposition and its application in CO2 adsorption. Ind. Eng. Chem. Res. 59, 16660–16668. https://doi.org/10.1021/acs.iecr.0c02687.

Zhu, W., Zhang, Y., Wang, X., Wu, Y., Han, M., You, J., Jia, C., Kim, J., 2021. Preparation and Comparative Study of Aerogels Based on Cellulose Nanocrystals and Nanofibers From Eucalyptus Pulp. https://doi.org/10.21203/rs.3.rs-1005528/v1.

Zhu, W., Chen, M., Jang, J., Han, M., Moon, Y., Kim, Junghwan, You, J., Li, S., Park, T., Kim, Jeonghun, 2024. Amino-functionalized nanocellulose aerogels for the superior adsorption of CO2 and separation of CO2/CH4 mixture gas. Carbohydr. Polym. 323, 121393 https://doi.org/10.1016/j.carbpol.2023.121393.

Zu, G., Shen, J., Zou, L., Wenqin, W., Lian, Y., Zhang, Z., Du, A., 2013. Nanoengineering super heat-resistant, strong alumina aerogels. Chem. Mater. 25, 4757–4764. https://doi.org/10.1021/cm402900y.